An Investigation into Hopper Design and Solid Friction Factor for Pneumatic Conveying of Indian Fly Ash

A Dissertation submitted
in the partial fulfilment of requirements
for the award of degree of

Master of Engineering

in

Thermal Engineering

by

Harpreet Singh

Registration No.: 801783006

Under the Supervision of

Dr. Gautam Setia (Assistant Professor, MED)

Mr. Atul Sharma (Lecturer, MED)

MECHANICAL ENGINEERING DEPARTMENT

THAPAR INSTITUTE OF ENGINEERING & TECHNOLOGY, PATIALA

July, 2019

CERTIFICATE

I hereby declare that the thesis entitled "**An Investigation into Hopper Design and Solid Friction Factor for Pneumatic Conveying of Indian Fly Ash**" is an authentic record of my work carried out as requirements for partial the award of the degree of **Master of Engineering** in **Thermal Engineering** at **Thapar Institute of Engineering & Technology, Patiala, Punjab** under the supervision of **Dr. Gautam Setia**, Assistant Professor and **Mr. Atul Sharma**, Lecturer, Mechanical Engineering Department, Thapar Institute of Engineering and Technology Patiala during July, 2018 to July, 2019. No part of the matter embodied in this project has been submitted to any other university or institute for the award of any degree.

Dated: 15/07/2019

Harpreet Singh

801783006

TIET, Patiala

It is certified that the above statement made by the student is correct to the best of my/our knowledge and belief.

Dr. Gautam Setia

Assistant Professor

Mechanical Engineering Department

TIET, Patiala – 147004

Mr. Atul sharma

Lecturer

Mechanical Engineering Department

TIET, Patiala - 147004

This thesis is dedicated to

my beloved father Kewal Singh and my mother Parkash Kaur

ACKNOWLEDGEMENT

I want to express gratitude to my supervisor Dr. Gautam Setia, Assistant Professor, Mechanical Engineering Department, Thapar Institute of Engineering and Technology, Patiala for continuous guidance and availability whenever is required. Apart from professional duties, his spark and realistic approach to any problem motivated me throughout.

I want to thank my co-guide Mr. Atul Sharma, Lecturer, Mechanical Engineering Department, Thapar Institute of Engineering and Technology, Patiala for moral support and guidance for thesis writing. His personality and working style helped me to teach various qualities like professionalism and multi-tasking.

I feel very fortunate to have the company of Dr. S.S. Mallick, Associate Professor, Mechanical Engineering Department, Thapar Institute of Engineering and Technology, Patiala. Dr. S.S. Mallick shared his experience and knowledge open heartedly. There are uncountable things that I have learned from such a great hard working personality.

I also owe support given by the staff of Central Workshop, Thapar Institute of Engineering and Technology for providing facilities like welding shop, carpentry shop and lathe machine, which helped several times for preparing an experimental setup.

Last but not least, I would like to thank my family, all friends and good wishers for their moral support and love.

ABSTRACT

Now a days, a variety of bulk solids are being conveyed through pneumatic conveying systems in different industries. In a thermal power plant, a huge amount of fly ash is conveyed pneumatically from the collection point to the intermediate or remote silos. The conveying system runs on the auxiliary power and hence should consume minimum energy. Inaccurate pipeline design and selection of the air movers (vacuum pump and compressors) can result in operational issues like pipeline blockage, less tonnage, and system wear. Moreover, accurate design of product feeders like hoppers and blow tank plays a vital role in ensuring the smooth discharge of the product in the conveying pipeline. This report presents the results of an experimental investigation to provide the crucial design parameters like hopper half angle, hopper outlet opening, and solid friction factor for a pneumatic conveying system. Two fly ash samples have been collected from two different thermal power stations from India. Jenike's design method was followed to design the hopper geometry for ensuring the smooth working of hoppers. Also, a new model has developed for solid friction factor for vacuum conveying setup.

Keywords – Vacuum conveying, flow properties, time consolidation, solid friction factor, fly ash.

TABLE OF CONTENTS

LIST OF TABLES

LIST OF FIGURES

NOMENCLATURE

Greek symbol

ρ_g	Gas density, kg/m^3
ρ_{lb}	Loose poured bulk density, kg/m^3
ρ_p	Particle density, kg/m^3
ρ_t	Tapped bulk density, kg/m^3
μ	Gas viscosity
λ_f	Air/gas only friction factor
λ_s	Solid friction factor through straight pipe
σ_1	Major principle consolidation stress, kPa
σ_c	Unconfined yield strength, kPa
δ_i	Effective angle of internal friction
φ_w	Wall friction angle

Abbreviations

Re	Reynolds number
Fr_g	Gas Froude number
Ar	Archimedes number
m*	Solid loading ratio
u	Pick up velocity, m s^{-1}
g	Acceleration due to gravity, m s^{-2}
ff	Flow function
ΔP_t	Total pressure drop
D	internal diameter of pipeline, m
K, a, b and c	Constants
HR	Hausner ratio
P	Porosity
CI	Compressibility index

D_c	Critical outlet diameter
HRW	Hard red wheat
SWW	Soft white wheat
PFT	Powder flow tester
ESP	Electrostatic precipitator
SEM	Scanning electron microscopy
NTPC	National thermal power corporation
PSD	Particle size distribution
APH	Air pre heater
MIV	Material inlet valve
SSA	Specific surface area
MIG	Metal inert gas

Chapter 1

Introduction and Objectives

1.1 Introduction

Pneumatic conveying has broad applications for bulk solids transferring in different sectors like fly ash conveying in thermal power plants, pharmaceutical powders conveying in the chemical industry, conveying different ingredients in the food processing industry and conveying of wide range of products in the packaging industry.

In India, 59% of total power generation is through coal-based thermal power plants (Rohit et al., 2017). Coal available in India for thermal power generation contains ash content as high as 40% by weight. The ash generated by this coal generally contains 80% of fly ash and 20% of bottom ash. This large amount of fly ash is conveyed pneumatically from collection point to remote silos. Thus, pneumatic conveying has huge application in field of fly ash transportation.

In a typical thermal power plant, fly ash along with flue gases produced in boiler travel through the economizer, air preheater (APH) and electrostatic precipitators (ESP). The fly ash gets collected in the economizer hoppers, APH hoppers, and ESP hoppers and the flue gases escape to the atmosphere through chimney. This ash is then fed into a pipeline from where it is conveyed to the next point (buffer hopper or remote silo) by using pneumatic conveying (pressure or vacuum).

A typical pneumatic conveying system contains an air mover, product feeder, conveying pipeline, and product separator (Klinzing et al., 2011). For smooth operation of any pneumatic conveying system, each component should designed such that there is no product blockage in the bins, hoppers, and pipelines by keeping the power consumption minimum. The capacity estimation of air mover (compressor or vacuum pump) must be accurate to avoid excessive

power consumption or product blockage. Each component through which the product flows or conveyed must be well designed to ensure maximum tonnage without product blockage. Designing of the hopper, which can act as transfer hopper, receiver bin, or blow tank is one of the critical parts of designing any pneumatic conveying system. The product flow properties play a vital role in deciding the design of hoppers and silos.

Inaccurate hopper designs can result into various flow problems like arching, ratholing, product flooding etc. Jenike has made a significant contribution in the field of hopper design by relating the product properties with hopper geometry. Today, a large number of researchers and engineers use Jenike design technique as a standard method to provide a tailor made hopper design for a wide range of bulk solids.

The accurate estimation of the pressure loss across a pipeline is important for a plant for its smooth and efficient operation. The pressure loss in a pipeline depends majorly on pipeline design and the product properties. The gas solid interactions during pneumatic are very complex and difficult to modelled fundamentally. Therefore, researchers and designers majorly rely on empirical modelling of solids friction factor, which is a key parameter in the estimation of pipeline pressure drop. For this, a product has to be conveyed in a test loop to obtain the input modelling data.

Thus, further research is required to accurately design the product feeder (hopper) and to estimate the solid friction factor for a given product to be conveyed through a pipeline configuration.

1.2 Objectives

The main aim of this thesis is to provide the data for a reliable design of the industrial hoppers and the pneumatic conveying pipelines. In view of this, the following objectives are undertaken:

i To investigate physical properties and flow properties of fly ash samples of two different thermal power plants.

ii To determine hopper geometry that includes a hopper half angle and critical outlet diameter for mass flow discharge.

iii To develop a model for predicting solid friction factor for vacuum conveying system.

Chapter 2

LITERATURE REVIEW

This chapter presents the research carried out by different researchers in field of flow properties, hopper design, and pneumatic conveying in the last few decades. Initial part of the chapter focuses on general discussion about the various components of pneumatic conveying, different types of systems, flow problems in hoppers and classifications of bulk solids based on Geldart's chart. The later part presents the research carried out by various researchers in the area of powder flowability, hopper design and pressure drop modelling.

2.1 Components of Pneumatic conveying systems

Any pneumatic conveying system contains the following four components as described by Klinzing et al. (2011):

(a) The prime mover which delivers conveying gas
(b) Product feeder for feeding, mixing and inducing
(c) Conveying pipeline
(d) Separator to separate the gas from product

The job of a prime mover is to deliver the conveying medium, i.e. air or particular gas. Prime mover can be a compressor, blower, vacuum pump or fan (as shown in Fig.2.1) as per the requirement of different products and operating conditions. A substantial amount of capital cost and maintenance cost goes to the prime mover. Selection of economic prime mover is a crucial task and requires estimation of the required gas flow rate and operating pressure.

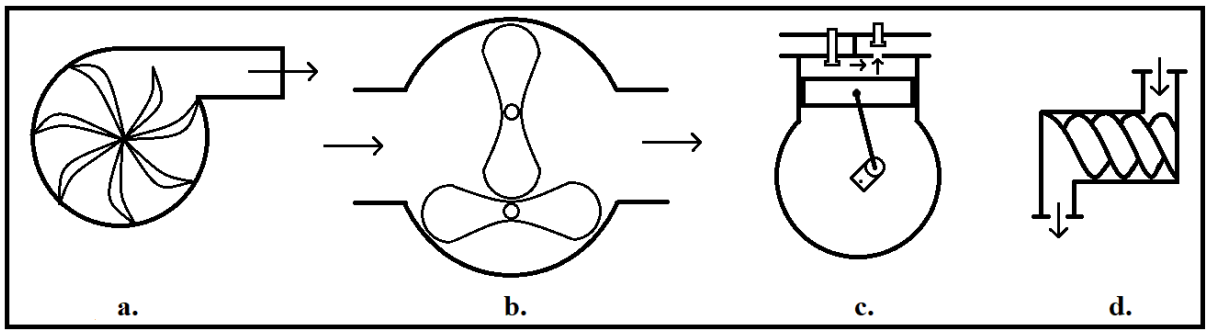

Figure 2.1: a. Fan, b. blower, c. Reciprocating compressor, d. Rotary screw type compressor

Feeding of the material to conveying pipeline is complicated to design, and a lot of problems occur in that zone. Proper mixing of conveying medium, i.e. gas with the bulk solid is required to avoid blockages in the conveying line. For mixing, blow tank can be used, and for feeding, venture, rotary valve or screw feed as shown in Fig.2.2 can used.

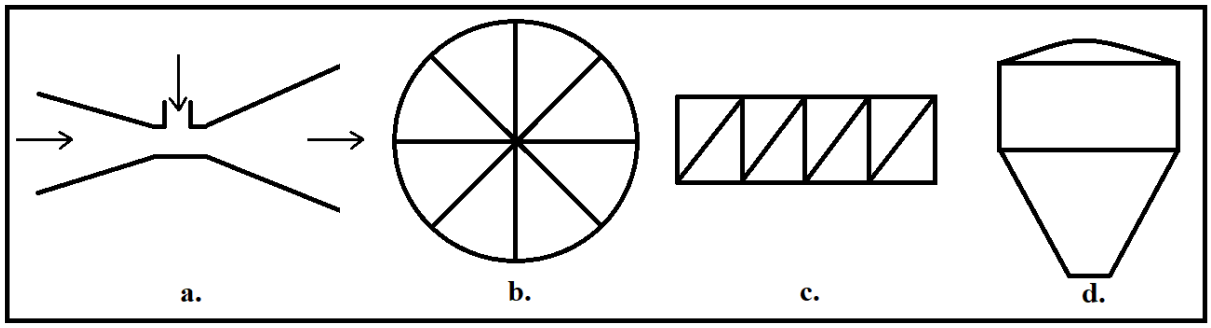

Figure 2.2: a. Venturi, b. Rotary valve, c. Screw feeder, d. Blow tank

A conveying loop generally includes straight pipeline, bends, diverts and flanges as shown in Fig.2.3. Material and size of pipe can be selected according to the type of material to be conveyed, tonnage, conveying distance and operating pressure. In a thermal power station, the conveying loop can have a length ranging from 500 m to 1500 m. On such scale majority of the pressure loss occurs in the straight horizontal line zone.

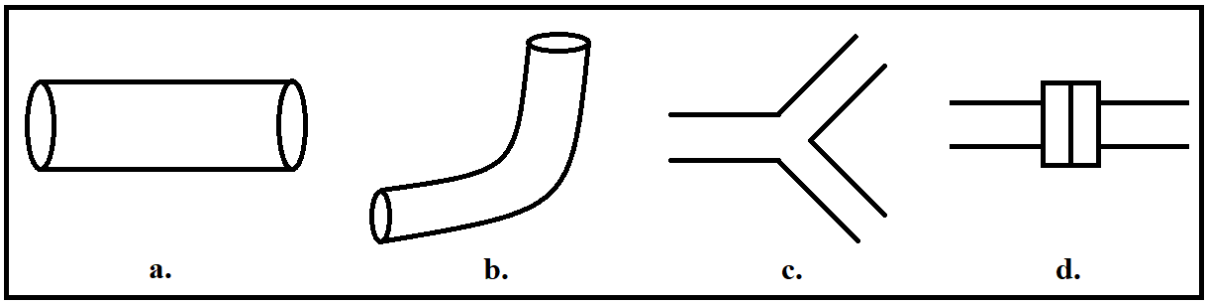

Figure 2.3: a. Pipe, b. Bend, c. Diverter, d. Coupling

The conveyed material must be separated from or conveying medium before storing in a storage tank or receiver bin. To disengage gas and product, bag filters or cyclones (as shown in Fig.2.4) are used generally. Separators are generally locate at the top of the storage tank.

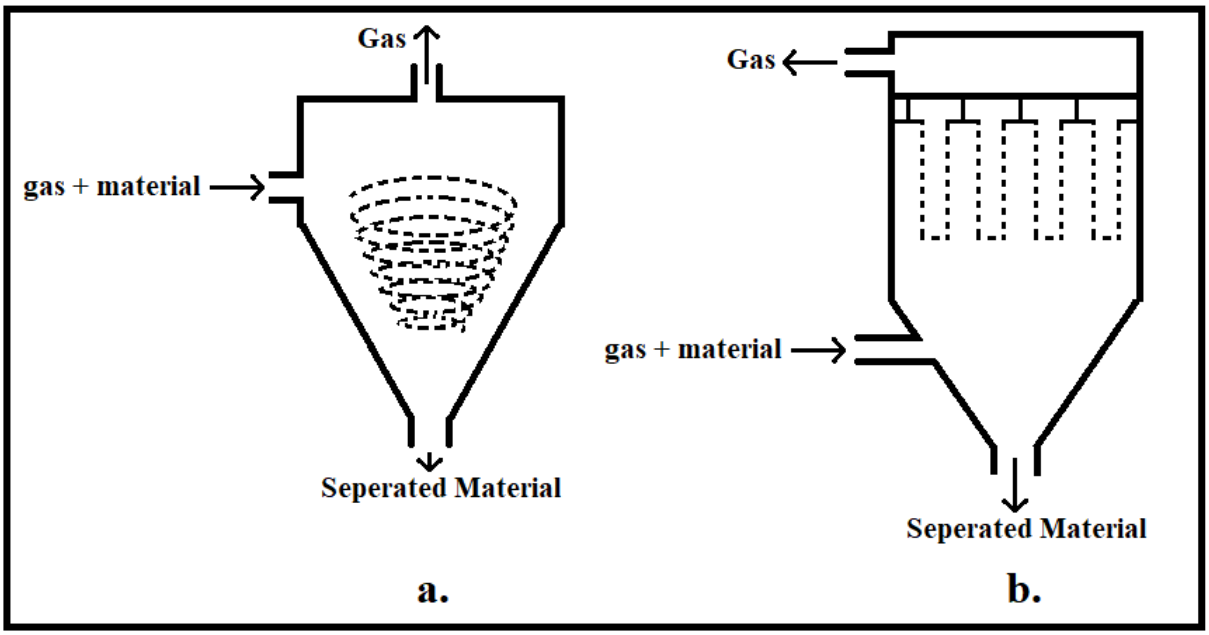

Figure 2.4: a. Cyclone, b. Bag filter

2.2 Types of Pneumatic Conveying systems

Basic pneumatic conveying systems can classified into three categories as described by Klinzing et al. (2011).

a) Positive pressure pneumatic conveying system,
b) Negative pressure pneumatic conveying system and
c) Combined negative and positive pressure pneumatic conveying system

Positive pressure pneumatic conveying system as shown in Fig. 2.5 conveys the material by maintaining pressure inside the pipe above atmospheric pressure. The pressure inside the pipe may reach up to 500 kPag for conveying of different particle size materials. The material present in the normal feeder is at atmospheric pressure (blow tank pressure remains above atmospheric pressure), and the conveying pipeline is pressurized. In this system, there is only one feeder or supply bin and have more than one receivers or discharge hoppers. Thus, this type of system has an extensive use in multiple discharge applications.

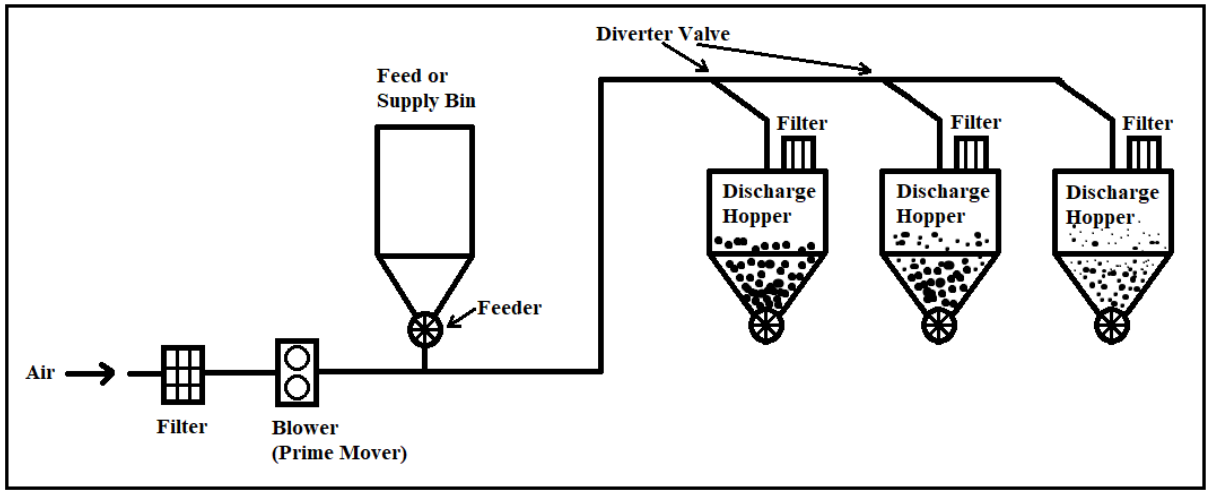

Figure 2.5: Basic positive pressure conveying system (Klinzing et al., 2011)

Negative pressure pneumatic conveying system as shown in Fig. 2.6 conveys material by maintaining vacuum inside the conveying pipeline. The pressure drop usually reaches up to 50 kPa, which limits the capacity of this type of systems. In this system, there can be multiple feeders or supply bins connected to one receiver or discharge hopper. As this system works in vacuum conditions, leakages don't produce dust or sprinkle. Thus these type of systems is suitable for conveying of toxic and hazardous materials.

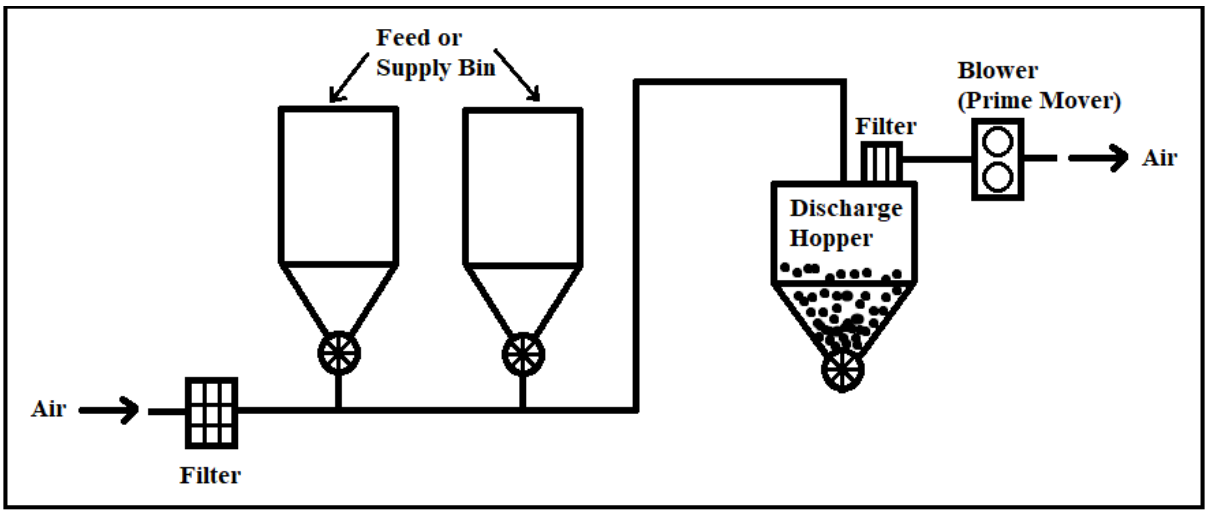

Figure 2.6: Basic vacuum conveying pneumatic system (Klinzing et al. 2011)

Combination of positive and negative pressure system as shown in Fig. 2.7 works as a push-pull system. In this system, there are multiple feeders and discharge hoppers. There is an intermediate hopper in between feeders add discharge hoppers. To match case specific requirements, separate vacuum and pressure blowers can be used as in Fig. 2.7 only one blower is shown.

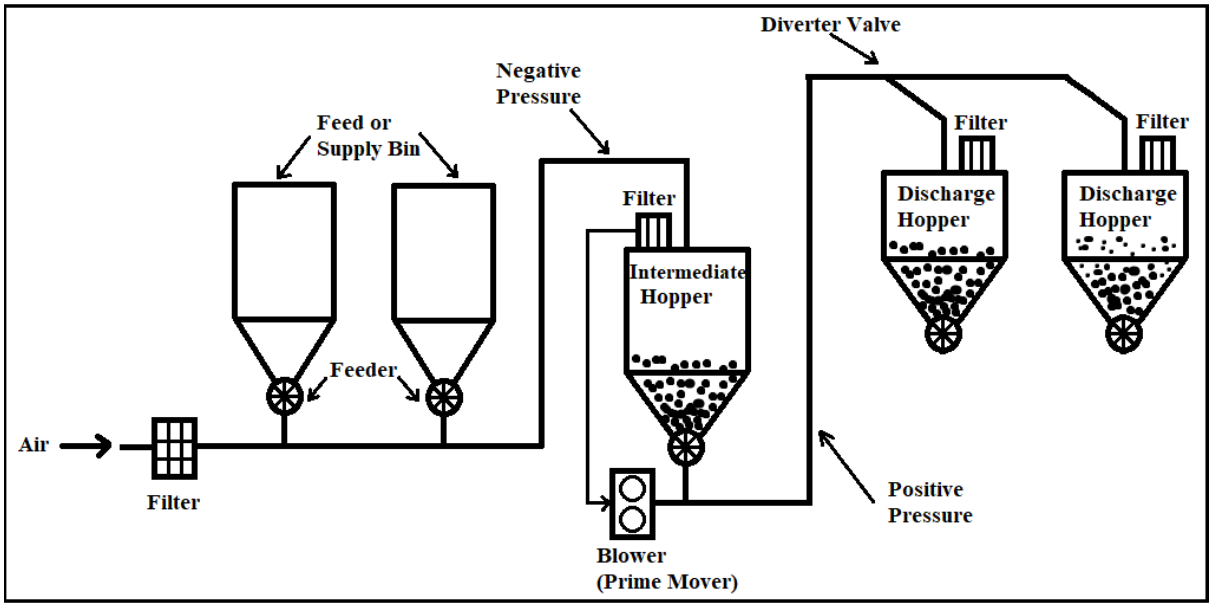

Figure 2.7: Combined negative and positive pressure pneumatic conveying system (Klinzing et al., 2011)

2.3 Flow problems in Hoppers

Hopper, as a part of any pneumatic conveying system or as a storage container, goes through several flow problems as described follows:

(a) Arching: - When the material to be conveyed is of larger particle size than arching may happen due to interwoven of particles. As shown in figure 2.8 a, at the outlet there is bridge like formation takes place which blocks the flow of material. Arching can also happen in case of small particle size due to high cohesion between particles of solid and compressive force due self-weight.

(b) Rat holing: - When the inner surface of the hopper is rough or shallow, the material start sticking along the walls. Stagnation zone builds along the wall. Material away from wall, i.e. towards center flows un-abruptly. The material along the geometrical axis of hopper moves continuously and looks like a rat hole as shown in Fig. 2.8 b.

(c) Funnel flow: - When rat holing takes place, the material in the stagnation zone remains as it is for a long time. As time pass on, the properties of material changes due to time consolidation. The material in the stagnation zone does not even move even if there is a space to flow. The flow of material looks like a funnel as shown in Fig. 2.8 c.

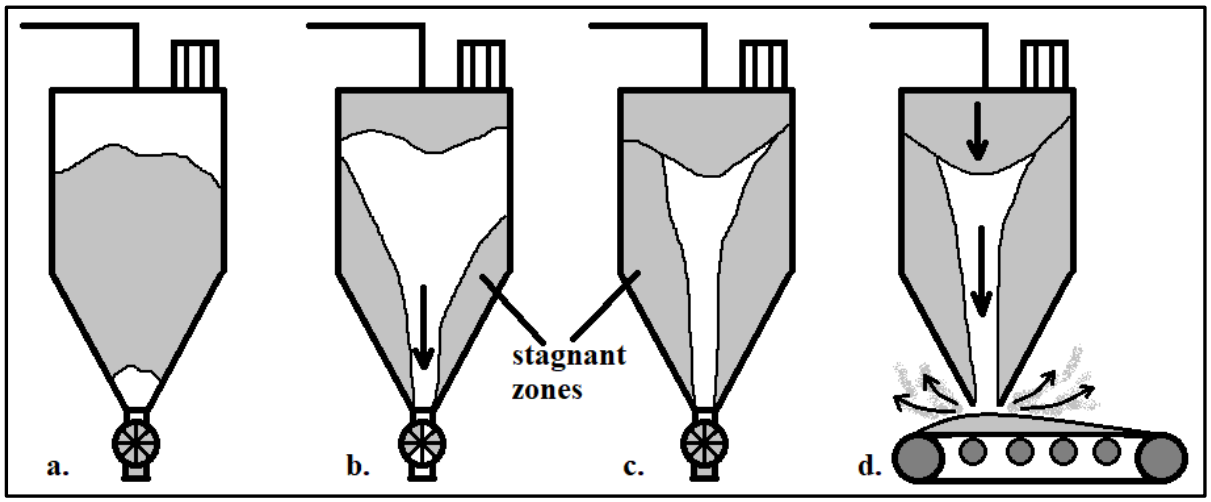

Figure 2.8: a. Arching, b. Rat holing, c. a funnel flow and d. flooding (Schulze, 2008)

(d) Flooding: - During funnel flow, when material enters the silo will not reside in a silo for much time as shown in Fig.2.8 d. Material first enters and first leave in no time, look like there is no use of hopper.

(e) Segregation: - Due to funnel flow, as material flow through the silo, segregation may take place as shown in Fig.2.9 e. Material having small particle size segregates towards geometrical axis of the silo and having large particle size segregates towards the wall. Due to segregation, the material comes out having different characteristics because particle size distribution changes.

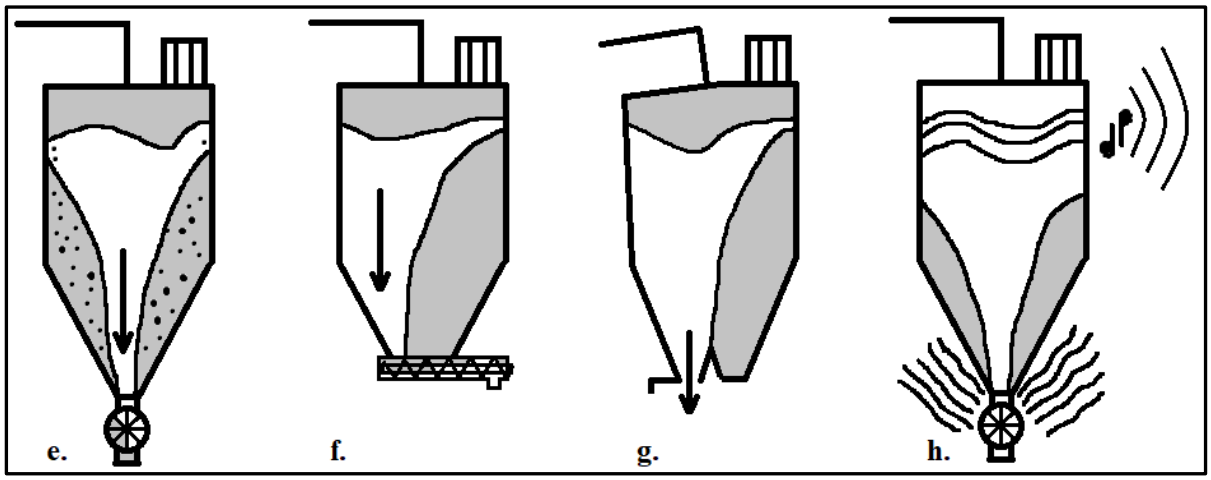

Figure 2.9: e. Segregation, f. Non-uniform discharge with screw feeder, g. Buckling caused by eccentric flow, h. Vibrations (Schulze, 2008)

(f) Non – uniform discharge: - When at discharge, screw feeder is in use, empty space for the flow of material is at the rear end of screw feeder. At the front side of screw feeder there is material moving along screw. The material enters in screw feeder from the rear end. Which results in non-uniform discharge as shown in Fig. 2.9 f.

(g) Buckling due to eccentric flow: - When there are multiple exits for material in silo and material is allowed to flow from one exit at a time. Then, the eccentric force start acting due to uneven load and may also result in buckling of silos as shown in Fig.2.9 g.

(h) Vibrations: - The vibrations and lot of sound produces during conveying due to the flow of bulk solids against different opposing forces. The opposing forces to conveying can be due to wall friction and internal friction. These vibrations can result to decline in lifetime of various components of conveying setup.

2.4 Geldart's classification for fluidization of powders

Geldart (1973) categorized powders according to its behaviour of flow after passing the fluidizing gas through a bed of powder. He divided powders into four groups i.e. group A, group B, group C, and group D by plotting available experimental data on density difference (ρ_p - ρ_f) and mean particle size (as shown in Fig. 2.10), explained as follows –

Group A includes powders having particle density less than 1400 kg/m^3 and small particle size. On supplying gas, these powders fluidized enough before bubbling starts. Bed of powders collapses very slowly after cutting off the supply of gas. Due to this nature, these powders can be conveyed easily in dense phase regime after giving some initial fluidization air in the product feeder.

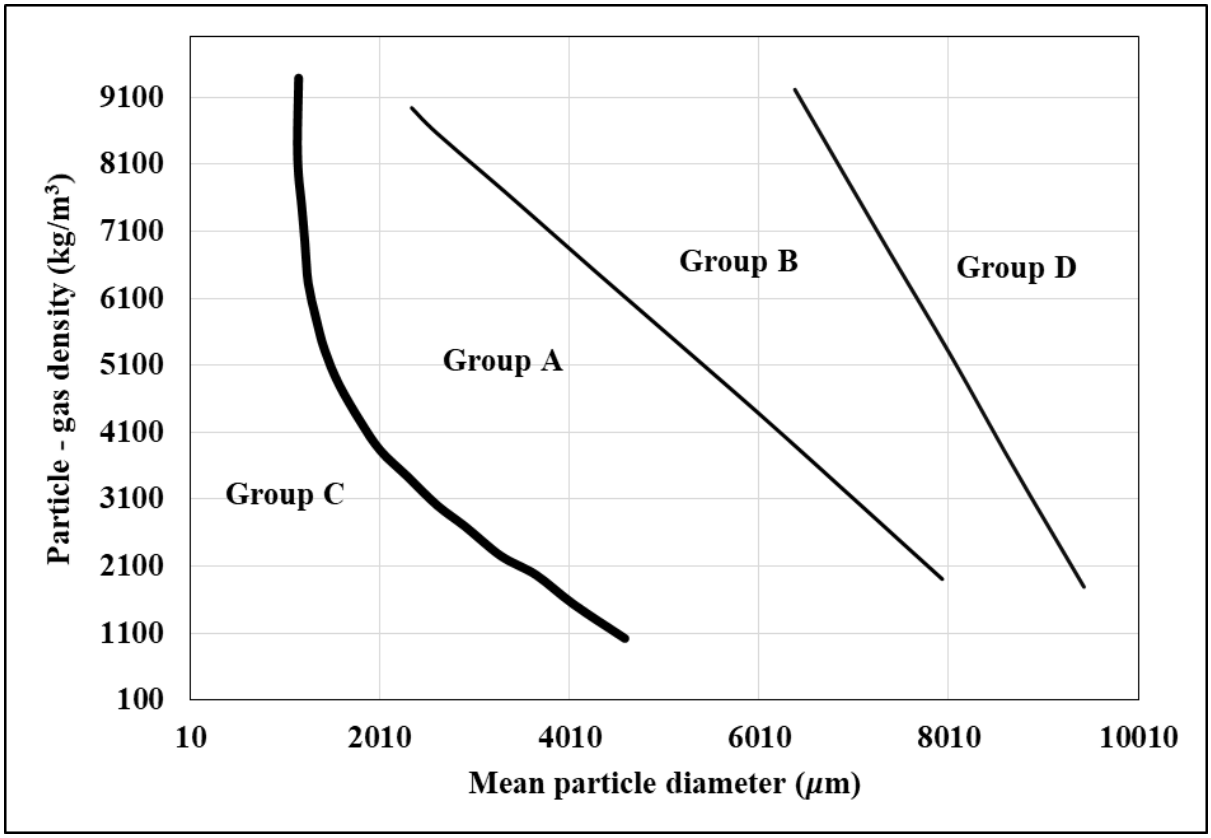

Figure 2.10: Categorization of powders for fluidization (Geldart, 1973)

Group B includes powders having particle density more than group A. Bubbling starts quickly at low fluidization velocity. These powders are unable to form bed because, after a particular

value of fluidization velocity, and fluidizing gas starts escaping in the form of bubbles. As a result, group B powders have less fluidization tendency than group A.

Group C includes very highly cohesive powders. When fluidization gas is passed, powder move as a whole bed instead of being fluidized. Thus, these powders are very difficult to get fluidized.

Group D includes powders having larger particle size and higher particle density than other groups. Poor fluidization takes place, and bubbles formed escapes very slowly.

2.5 Literature Review

Garg et al. (2018) did investigation on flow behaviour of calcium sulphate (d_{50} = 47 µm) and dicalcium phosphate (d_{50} = 23 µm). They found di-calcium phosphate is more cohesive than calcium sulphate powder due to high porosity and large tapped density of the dicalcium phosphate. Time consolidation effect on both the powders was analyzed and it was found that time consolidation has a stronger effect on calcium sulphate than di-calcium phosphate. They found that calcium sulphate is easily flowable as compared to di-calcium phosphate. Di-calcium phosphate requires larger hopper outlet critical dimension than calcium sulphate. They developed a mathematical model to determine cohesion (kPa) and unconfined yield stress (kPa). The developed mathematical model was verified by comparing with experimental results of pharmaceutical powders, i.e. magnesium tri-silicate, paracetamol, lactose, and starch, having a particle size less than 100 µm.

Bian et al. (2015) compared between hard red wheat (HRW) and soft white wheat (SWW) flour for physical and flow properties. Their investigation showed that the particle shape and particle size distribution affect the flowability of powders. HRW and SWW had similar particle size but different particle size distribution. Results showed SWW flour has higher aeration ratio, higher compressibility, and low permeability than HRW flour. SWW flour found more cohesive than HRW flour, thus require lesser hopper half angle.

Salehi at al. (2017) made a comparison between Jenike shear cell tester, Schulze ring shear tester, and Brookfield powder flow tester (PFT) for same applied load conditions. According

to Jenike's classification, dolomite lime lied in cohesive range, calcium lactate lied in free-flowing range, and calcium carbonate lied in very cohesive range. These three samples tested at mentioned three flow property testers and their experimental results have compared. Three testers were compared by measuring different flow properties, i.e. raw shear stress time series, yield loci points, angle of friction, cohesion, and unconfined yield strength. They found that Brookfield PFT is less appropriate for testing of free-flowing materials. For cohesive and slightly compressible materials, these three testers produced similar results.

Takeuchi et al. (2018) studied the effect of particle size and particle shape on the flowability of powders. Flowability of powders estimated through carr index, shear test and dynamic flow test. Experimentation on which samples has done includes fine crystalline mannitol powder, eight commercial types of mannitol granules and four types of mannitol mixture granules having particle size varies from 36.6 to 317.8 μm. Results have shown that as the shape of granules become spherical, flowability improves. Results also have shown that as particle size increases, flowability improves as carr's index increases. They concluded that particle size has more impact on Carr's index than particle shape. Shear stress and angle of internal friction were more impacted by particle shape than particle size.

Rohilla et al. (2018) experimentally investigated the effect of particle size of fly ash on its flowability. Experimentation done on seven samples of fly ash (particle size varies from 21 to 139 μm) taken from different ESP hoppers. Powder flow tester (PFT) based on Jenike's methodology was used to determine different flow properties , i.e. yield locus, flow function curve, wall friction angle, and angle of internal friction. Power function model was developed to design critical parameters of hopper, i.e. hopper half angle and outlet diameter. The dependency of hopper half angle on wall friction and flow properties of powder was utilized to develop a model for hopper half angle. The experimental analysis has shown that with an increase in particle size, cohesion decreases. Similarly, variation of different flow properties for physical properties was analyzed by plotting experimental data on graphs.

Lee et al. (2015) did experimentation on soybean powders with different particle sizes varying from 740.6 to 1448.66 μm. Flow properties, which include flow function, the effective angle of internal friction and angle of wall friction have resulted in powder flow tester (PFT). Trends of flow properties for particle size and particle shape analysed. Results have shown that as the particle size of powder decreases, flowability decreases, which require larger hopper half angle

and larger critical outlet diameter. Particle size variation not shown ordered variation with internal friction angle due to the influence of other physical properties like particle shape might be in this case. Results have also shown that with an increase in circularity of particle, internal friction angle decreases, i.e. flowability reduces.

Fitzpatrick et al. (2004) studied the flow properties and physical properties of thirteen different food powders , i.e. Salt 140, Tea, Salt 200, Tomato, Maltodextrin, Sugar 140, Soy flour, Cocoa, Non-fat milk, Corn starch, Wheat flour, and Cellulose. They found that particle size and moisture content varies flowability of food powders, but no direct relation found. They resulted that for deciding flow properties of the powder, cohesion forces and adhesion forces between particles and wall plays an important role. Jenike's methodology for calculating hopper design dimensions, i.e. hopper half angle and opening diameter considered as standard but for very cohesive powders, results might not always as expected. They found wall friction as vital parameter to predict whether the flow of powders in a hopper is mass flow or funnel flow.

Leung et al. (2016) did investigation on the precision of ring shear tester for measuring flow properties of different powders. They did experimentation on six samples of pharmaceutical powders, i.e. Micro-crystalline cellulose (PH 101), Micro-crystalline cellulose (PH 105), Mannitol (Delta M), Lactose Monohydrate (Fast Flo 316), Granule 1 (from roller compaction) and Granule 2 (with high shear wet granulation). They found flow function measurements taken from a ring shear tester are influenced by different flow properties of the powder. Cohesion showed great influence on the measurement of flow function. Ring shear tester gave less precise results for testing the powder having lesser cohesion value. Friction angle of powders did not shown any considerable effect on flow function measurement. Experimental results have shown that if we do experiments on shear tester at different pre-consolidated stress values, no improvement will happen in precision.

Mallick et al. (2009) did modeling to predict minimum transport boundary. They found that it is crucial to find boundary condition at which flow changes from stable to unstable. Accuracy in predicting minimum transport boundary decides the quality of flow and economy in energy consumption. They also found that existing methods of estimating minimum transport boundary were not much accurate; thus, they developed a new method using a Froude number. They conducted experiments on twelve different powders (particle size varies from 7 to 55 μm)

by conveying through pipes of different diameter and length. They also found that pneumatic conveying of powders under dense phase is preferred due to improved efficiency, less volume of gas required, less power consumption, better product quality, and enhanced workplace safety. However, models they found for dense phase conveying were mostly empirical and based on particular pipe dimension and flow conditions. Also, these models not tested under scale-up conditions. They resulted Froude number is a useful parameter for minimum transport criteria.

Setia et al. (2015) found Froude number as an essential criteria for an estimation of minimum conveying velocity for different dimensions of pipe. They also found that pressure tapping points make a significant difference in pressure drop and effects on the mechanism of flow along the flow direction. They introduced a new approach for modeling solid friction factor by using volumetric loading ratio term. Models developed by them shown in Eq. (2.1) as follows:

$$\lambda_s = K.(m^*)^a.(Fr)^b.\left({\rho_f}/{\rho_s}\right)^c \tag{2.1}$$

Setia et al. (2015) did modeling for estimating minimum transport boundary for dense-phase pneumatic conveying systems. Experimental data for 22 different powders conveyed through 38 different pipe sizes was collected. They did modeling by taking gas Froude number as a power function of solid loading ratio in one model and as a power function of solid loading ratio and particle Froude no. in another model. They found that models present at that time were still limited to small range of products and pipe sizes, needs to be tested for precision and scale-up conditions. Models developed by them validated by using experimental data of 3 products conveyed through 5 different pipe sizes.

Cabrejos et al. (1994) did an experimental study for defining pickup velocity and saltation velocity. Through different experimental observations, he concluded that the velocity of conveying gas at which fluidized powder suspension particles starts to separate themselves from suspension and starts settling down, called saltation velocity. The velocity of the gas at which particles present at rest at pipe bottom start moving to form a suspension. The concluded

that to calculate minimum conveying velocity, atmospheric pressure should taken into consideration.

Wypych et al. (2003) did investigation on pneumatic conveying characteristic curves for granular materials. They divided PCC's into four zones i.e. Blockage, Dense-phase, Unstable zone, and Dilute phase, as shown in Fig.2.11.

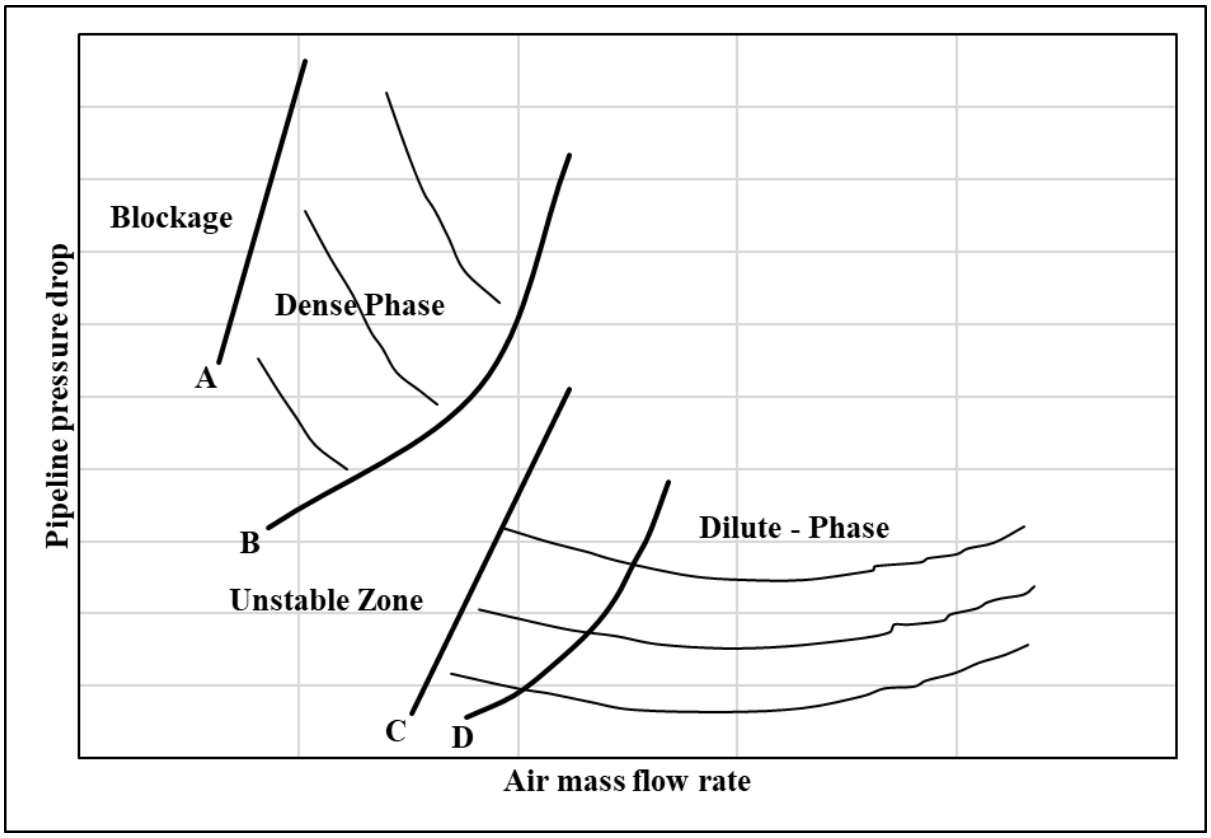

Figure 2.11: PCC for granular material [P.W. Wypych, 2003]

Between boundaries A and B, the material will flow like a slug moving slowly. Between boundaries C and D, the material will flow as suspended particles as a whole and no deposition of particles occur at the bottom of the pipe. Between boundaries B and C, the flow will be unstable, and fluctuations in air pressure along with pipeline vibrations occur.

Kalman et al. (2005) collected a large amount of experimental results of about 24 materials of different physical properties for pickup velocity measurement. They found a relationship between the Reynolds no. and, also Archimedes no. for representing pickup velocity. Three zones defined for different pickup velocity requirement for different particle size. In the first zone, as particle size increases, pickup velocity also increases, and cohesive force is negligible. In the second zone, pickup velocity increases as particle size decrease because of cohesive force come into play. In the third zone, pickup velocity remains constant because fine particles move as the whole group due to high cohesive forces.

Zhou et al. (2018) did an experimental study on swirling effect on pneumatic conveying of lump coal particles having a size of range 5 – 15 mm. They examined available literature related to different aspects that will affect pickup velocities like axial flow, tangential flow, swirling effect and oscillating flow, etc. They developed a new type of swirling generator for experimental purpose. They found three main factors that directly influence swirling effect, i.e. total inlet flow rate, the measurement position, and the tangential flow rate. They found pickup velocity values by using weight loss method. Results shown that by using the swirling effect, pickup velocity first increases but then decreases significantly. Thus swirling effect found useful in reducing power requirement for pneumatic conveying of lump coal particles.

Hu et al. (2014) did experiments on Rosy bentonite by conveying it through bending slits to study blockage condition. Effect of different parameters like bending angle of a slit, pressure drop, conveying pressure and superficial velocity, etc. on blockage boundary has investigated by plotting graphs between these parameters. The experimental study resulted that on increasing bending angle, solid loading ratio increases, and conveying pressure decreases, also, on increasing superficial air velocity, solid mass flow increases. Also, as total conveying pressure increases, blockage condition shifts towards high solid mass flow rate and lower superficial velocity.

Hu et al. (2015) did an experimental study on powder having particle size 48μm in horizontal slit for predicting blockage boundary. As per the experimental study, they concluded that on increasing superficial air velocity, solid mass flow rate increases. Also, on increasing

conveying pressure, solid mass flow rate at the blockage boundary increases. At constant conveying pressure if superficial air velocity, solid loading ratio at blockage condition first decreases to a minimum and then start increasing. They also resulted that on increasing conveying pressure, solid loading ratio at blockage condition increases.

Cenna et al. (2014) did a study on wear on the pipeline for pneumatic conveying of different particle size powders. They took samples of pipelines and by using Scanning electron microscope (SEM) images examined their surface. They found that wear of pipe takes place by both abrasion and erosion. They also found that wear happened by fine particles is majorly due to erosion and wear happened by large particles is majorly due to abrasion. As a result, wear by erosion due to high velocity conveying was found an important factor for the service span of any pneumatic conveying system.

Pan (1999) did experimental investigation for different modes of flow for bulk solids through pneumatic conveying and their relation with material properties. Three types of flow modes was observed , i.e. dilute phase to dense phase smooth transition, unstable slag flow with dilute phase and only dilute phase. They found that modes of flow highly depend on those properties of the material which include particle-air interaction, which further depends on particle properties. By plotting, loose poured bulk density vs. mean particle size for different materials, three groups of particles as already mentioned modes have resulted. Also indicated about exceptions that might happen due to unusual physical properties and put these materials in only dilute phase flow group.

Rabinovich et al. (2011) did an experimental and theoretical study on the flow behaviour of fluidized materials of different particle sizes (0.026 – 1.84 mm) in the vertical pipeline. They introduced different flow types , i.e. for dense phase flow; flow can be a separate plug, particle rain, fluidized flow, bubbly flow, slug flow, or turbulent type. Similarly, for dilute phase flow, flow can be of cluster flow, annular flow, or suspension flow type. From literature, they found Reynold no. and Archimedes no. as most precise parameters for different flow transition velocities in a vertical system. They also introduced void fraction and solid loading concentration, which they mentioned as influential parameters for vertical flow in pneumatic

conveying. For modeling they used modified Reynold no. as a power function of Archimedes no. to include the effect of solid loading and void fraction.

Chapter 3

Material and Methods

For the experimental investigation, the vacuum conveying test facility and powder flow tester available in the Laboratory of Particle and Bulk Solids Technology of the Mechanical Engineering Department at the Thapar Institute of Engineering and Technology, Patiala, Punjab (India) were used. This chapter gives a detailed description of the test setup used for the experimental investigations.

3.1 Vacuum conveying setup

3.1.1 Components and their specification

Receiver Bin – Conical shape hopper used as receiver bin having water fill volume capacity of 0.8 m^3. Hopper half angle was 30° and fabricated by sheets of mild steel. Receiver bin was supported on four shear beam load cells. These load cells were connected to a data logger for recording readings at the rate of 1 reading/ 5 sec. Receiver bin was assembled in such a way that all the load was equally divided on four load cells, and no other load either eccentric or along the axis was there. At the outlet of receiver bin, there is a manual isolation valve (knife gate valve) followed by pneumatically controlled double disk valve.

Transfer Hopper – Transfer hopper was having the conical shape with the water fill volume of 0.4 m^3. Transfer hopper was supported on the three shear beam load cells which connected to a data logger for collecting load data at the rate of 1 reading/ 5 sec. The outlet at the bottom of receiver bin was connected to inlet of the transfer hopper with double disk valve in between.

Vacuum Pump – Liquid ring type vacuum pump of 29 BKW manufactured by PPI Pumps PVT LTD was used to generate a vacuum in the receiver bin. Power required to run vacuum pump transferred through 'V' belt drive from 37 kW motor. For feeding water into the vacuum

Loop section	Length (m)
A	7
B	10
C	7
D	15
E	17
F	2
G	4
Total	62

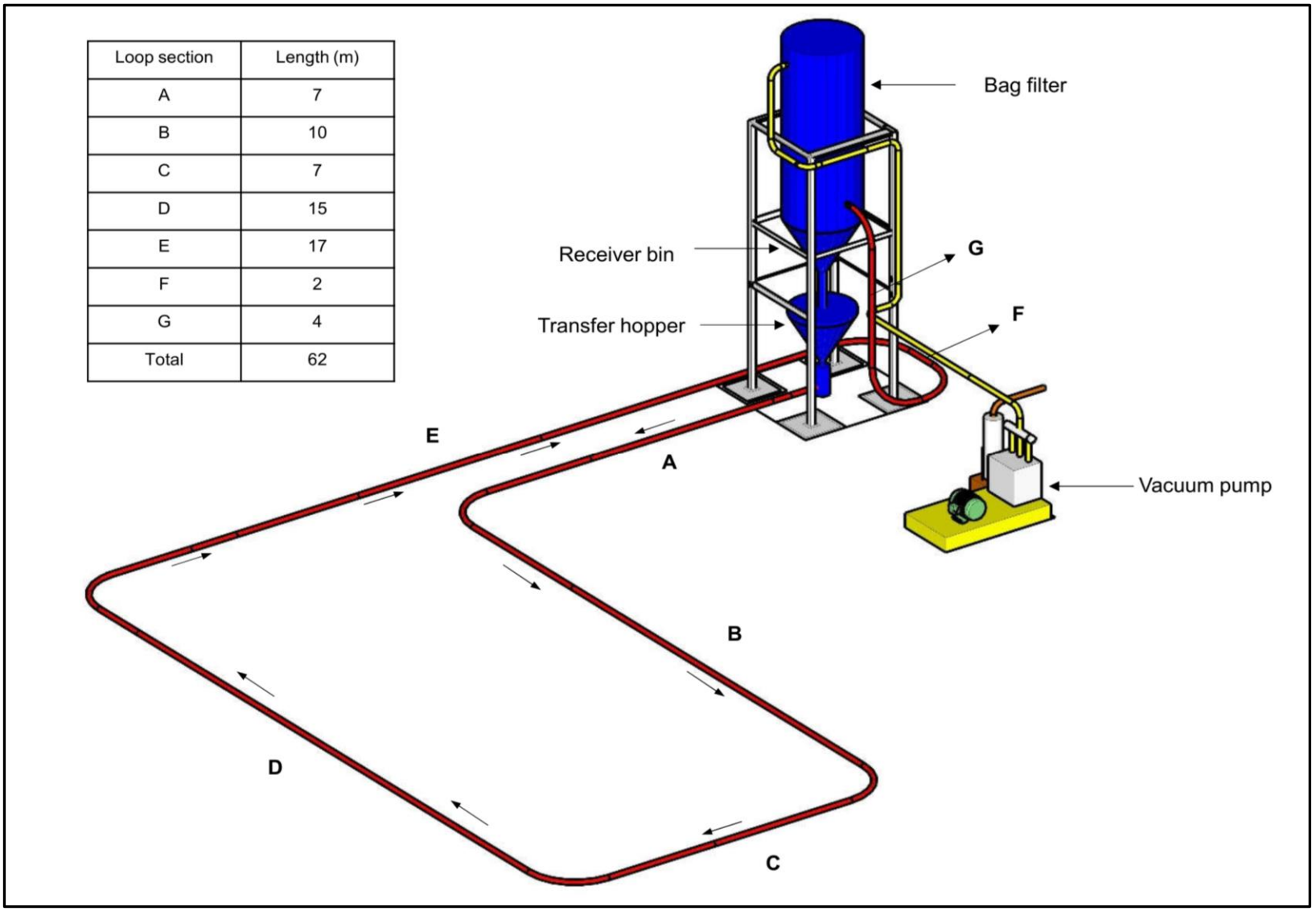

Figure 3.1: Experimental setup for vacuum conveying of fly ash

pump, a centrifugal pump of 0.75 KW and 2800 rpm was used.

Pipeline – A closed loop of pipeline having a total length of 62 m installed for conveying. Pipeline consisted of one vertical section of length 4 m, six horizontal pipes and six 90° bends as shown in Fig.3.1. The pipeline was of constant internal diameter of 105 mm throughout and made of mild steel.

Load cell – Shear beam type load cells of Model 65023 has used for taking readings of transfer hopper and receiver bin weight. These load cells give a full scale output of 3 mV/V and manufactured by nickel plated alloy tool steel.

Data Logger – A data logger (dataTaker DT80) was used to record the pressure and load readings during the conveying trials.

3.1.2 Working of Vacuum conveying setup

The setup used for the vacuum conveying trials is shown in the Fig.3.1.

The following tasks were performed to get the system ready for the conveying trials :

a. Fly ash sample (400 kg) was filled into the receiver bin through a utility hole.
b. Calibration of all load cells was done through standard procedure.
c. Compressed air was filled in the air reciever at a pressure of 6 bar for operating all the pneumatically operated valves.

As the experimental setup got ready, the following steps were performed:-

i. First, the material inlet valve (MIV) gets opened so that material from the receiver bin will come to transfer hopper. From load cells connected to the data logger, reading of empty receiver bin that was 2080kg, indicated that all the ash had fallen into transfer hopper.

ii. Now, the material inlet valve gets closed. Reading from transfer hopper load cells also shown that all the ash has fallen into the hopper.
iii. Turn ON vacuum pump, to maintain vacuum in receiver bin and pipeline. From vacuum transducer, we get reading of vacuum. Vacuum maintained for experiments done varies from 160 to 240 mm of Hg.
iv. Now the material outlet valve was opened and the ash started to get conveyed from transfer hopper to receiver bin through a pipeline.
v. Load cell gives the tonnage readings to the data logger for a particular conveying cycle.
vi. When load cell readings for transfer hopper shows 896 kg, it indicated all the ash got conveyed, and the transfer hopper is empty.

All the above steps were performed for one cycle and were repeated for a number of experiments.

3.2 Test Samples

The samples of APH fly ash taken from two different super thermal power plants located in India. The first sample named APH sample A, has taken from a coal-based power plant of capacity 1820MW. The second sample, called APH sample B, has taken from coal based power plant of capacity 2320MW. These samples were taken during the running condition of a power plant and carried through water-proof bags to the testing facility. The quantity of the fly ash sample collected from each thermal power plants was 500 kg (sufficient enough to run the trials).

3.3 Physical Properties

Particle size distribution (PSD) and Specific surface area

Particle Size Distribution of the fly ash samples was performed using Malvern Mastersizer 2000. It is the most widely used instrument to measure particle size and specific surface area, manufactured by Malvern Instruments, Worcestershire, UK. Specification of this instrument includes particle size measurement range of 0.020 to 2000μm having refractive index 1.52 and

absorption index of 1. This instrument worked on the principle of laser diffraction and used to measure particle size and specific surface area of samples.

Loose pored bulk density

Loose poured bulk density is the density measured when the sample is at aerated state. For measuring, the sample is first passed through sieve size of 1mm and then collected in measuring cylinder. For calculating sample weight, the weight of hollow cylinder subtracted from the weight of cylinder containing sample. The volume of sample noted from cylinder dimensions. Loose poured bulk density measured by using formula –

$$\rho_b = \frac{Mass\ of\ sample}{Volume\ of\ loose\ sample} \tag{3.1}$$

Particle density

For measuring particle density, water displacement method has used. Amount of water taken in measuring tube and its mass and volume noted down. Then, the amount of powder put into a tube containing water and wait till air bubbles collapses and particles settled down. Again, note water and volume noted down –

$$\rho_p = \frac{Mass\ of\ the\ sample\ and\ water - mass\ of\ the\ water}{Volume\ of the\ sample\ and\ water - Volume\ of\ the\ water} \tag{3.2}$$

Tapped bulk density

It is an increased bulk density attained after mechanically tapping a container containing the powder sample and found by formula as shown below –

$$\rho_t = \frac{mass\ of\ the\ sample}{Tapped\ volume\ of\ powder} \tag{3.3}$$

The minimum packed volume thus achieved depends on no. of factors includes particle size distribution, true density, particle shape and cohesiveness due to surface forces. Therefore, the tapped density of material have an influence on flow behavior Abdullah et al. (1999) and compressibility of powders.

Porosity and Compressibility index

Porosity is a measure of void spaces in a material. Compressibility index or Carr index is the measure of extent up to which any powder can compressed and a useful parameter to characterize powders Carr (1965). Formulae used to measure porosity and compressibility index was –

$$Porosity = 1 - \frac{\rho_{lb}}{\rho_P} \tag{3.4}$$

$$Compressibility\ index = 100\left(1 - \frac{\rho_{lb}}{\rho_t}\right) \tag{3.5}$$

Hausner ratio

Hausner ratio is the ratio of tapped bulk density to loose poured bulk density and the formula used to find it was –

$$Hausner\ ratio = \frac{\rho_t}{\rho_{lb}} \tag{3.6}$$

Particle shape

The particle shape of given samples examined with the help of Scanning Electron Microscopy (SEM) technique. For SEM images facility at Sophisticated Analytical Instruments Laboratory

at Thapar Institute of Engineering and Technology, Patiala used. An instrument named JSM-5510 Scanning Electron Microscope manufactured by JEOL Ltd, Tokyo, Japan was used at 15KV of accelerating voltage.

3.4 Flow properties

Flow properties, i.e. flow function, wall friction angle, and bulk density were measured with the help of Powder Flow Tester (PFT) as shown in Fig. 3.2. The testing equipment was manufactured by Brookfield Engineering Laboratories, Inc., Middleboro, MA, USA. This test facility was available at Laboratory for Particle and Bulk Solids Technologies, Thapar Institute of Engineering & Technology, Patiala. The method used for testing sample on PFT consisted following steps –

i. There are two types of vanes: Standard vane lid and Standard wall friction lid made of 304 SS and have a 2B surface finish. For flow function testing, vane lid has been used which was divided into 18 equal compartments through vanes. For wall friction test, wall friction lid has been used, which has got smooth surface for sliding over powder.

ii. For preparing the sample, there is a trough made from aluminium. A trough was of annular shape to contain powder and perforated at the bottom so that powder particles cannot slide at the bottom. Inner catch tray which gets fitted at the centre, was rotated by hand to prepare a sample. It has shaping blade (restricted to axial movement) fixed at the center was rotated by hand for spreading powder equally in annular space. Care must taken that flat profile of shaping blade is for wall friction test and curved profile is for a flow function test.

iii. Subtract the weight of vane from the weight of vane containing powder to get the weight of the only sample. Weight of sample put as input to pro software before starting test.

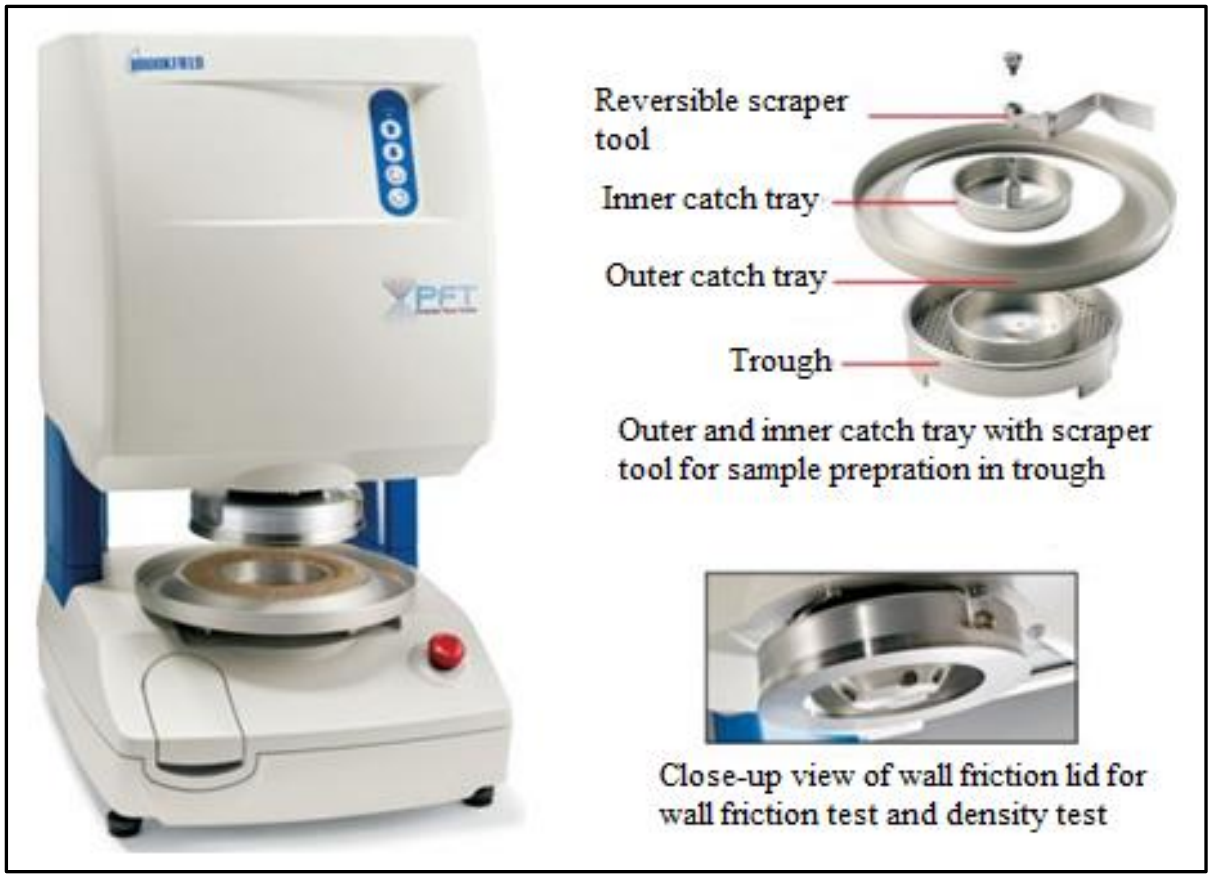

Figure 3.2: Image of Powder Flow Tester

Flow function

Flow function has been calculated using PFT based on Jenike's method (Jenike, 1964 and Schulze, 1990). To find flow function, values of unconfined failure stress (σ_c) for different values of major principal consolidation stress (σ_1) have required. As shown in Fig. 3.3, two Mohr circles have required, one for the value of unconfined failure strength and other for the value of major principle consolidation stress. First, the sample was applied by a particular value of normal stress from which one Mohr circle has drawn. Then at that normal stress, shear stress has applied up to failure of the sample. From this value of shear stress and normal stress, we got other Mohr circle. This method has repeated for different values of normal stress to develop flow function curve.

Flow function (ff) can be found by using formula: -

$$ff = {}^{\sigma_1}/_{\sigma_c} \tag{3.7}$$

Standard classification (Jenike, 1964) of flow function values has been used for powder flowability as shown below:-

ff<1	Non-flowing
1<ff<2	Very cohesive
2<ff<4	Cohesive
4<ff<10	Easy flowing
10<ff	Free flowing

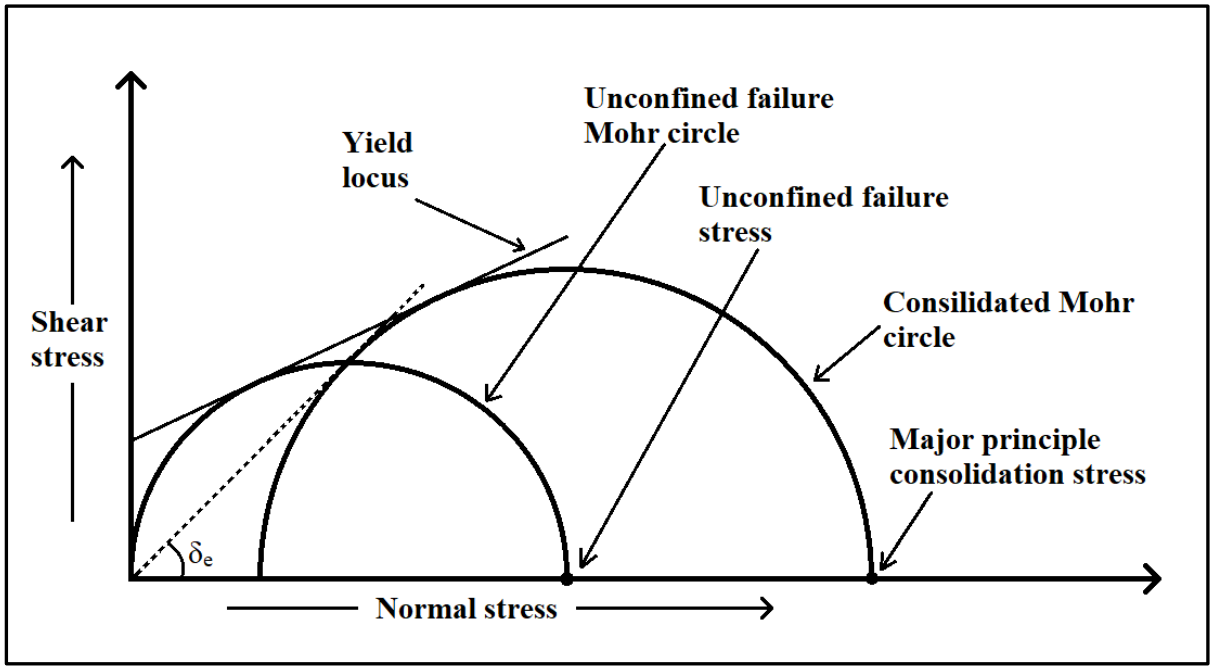

Figure 3.3: Schematic diagram of Mohr circles for determining unconfined failure stress, major principle consolidation stress and yield locus

Bulk Density

Bulk density has measured by using PFT at different values of normal stress varies from 0.112 to 4.946 kPa. Bulk density measured was compacted bulk density because it measured under normal stress. For bulk density testing, wall friction lid has used, and trough holds 230 cm^3 volume of sample.

Effective angle of wall friction

Wall friction angle is the slope of the line drawn from origin to maximum value of shear stress on the Mohr's circle drawn for wall shear stress and normal stress. It was determined for different values of normal stress and varies from 0.483 to 4.336 kPa on PFT.

Effective angle of internal friction

Effective angle of internal friction is the slope of a line drawn from origin and tangent to the Mohr's circle for consolidation stress. It was determined on PFT with normal stress values and varies from 0.682 kPa to 9.28 kPa. Vane lid has been used, and trough holds a sample size of 263 cm^3.

Chapter 4

Results and Discussion

4.1 Physical properties

Various physical properties of APH ash sample A and APH ash sample B shown in Table 4.1. APH ash sample A is of larger mean particle size than APH ash sample B. The larger particle size of APH ash sample A results into higher van der waals forces between particles but due to lesser particles in contact with each other results lower strength (Schulze, 2008). The smaller particle size of APH ash sample B can result to lower flowability (Lee, 2015) and also influence other flow properties like bulk density and compressibility (Barbose-Canovas et al., 2005). Span for APH ash sample B is larger which signifies broader particle size distribution. APH ash sample B has a higher specific surface area which can result to lower flowability and higher adhesion with wall. Porosity of APH ash sample A ash is more than APH ash sample B, which results to higher compaction due to self-weight when stored in any [Crowley et al., 2014].

Table 4.1: Physical properties of APH ash sample A and APH ash sample B

Property	**APH ash sample A**	**APH ash sample B**
d_{10} (µm)	53.644	29.02
d_{50} (µm)	142.053	96.107
d_{90} (µm)	288.6	217.825
S	1.654	1.965
SSA (m^2/g)	0.0677	0.124
ρ_{lb} (kg/m^3)	986	800.67
ρ_p (kg/m^3)	2407.96	1757.78
ρ_t (kg/m^3)	1332.56	1051.23
HR	1.3514	1.313
P	0.59	0.544
CI	26.007	23.835

The particle size distribution of the sample A and sample B of APH has shown in the Fig. 4.1. The PSD results shows APH sample A has higher mean particle size than APH sample B as mentioned in table 4.1.

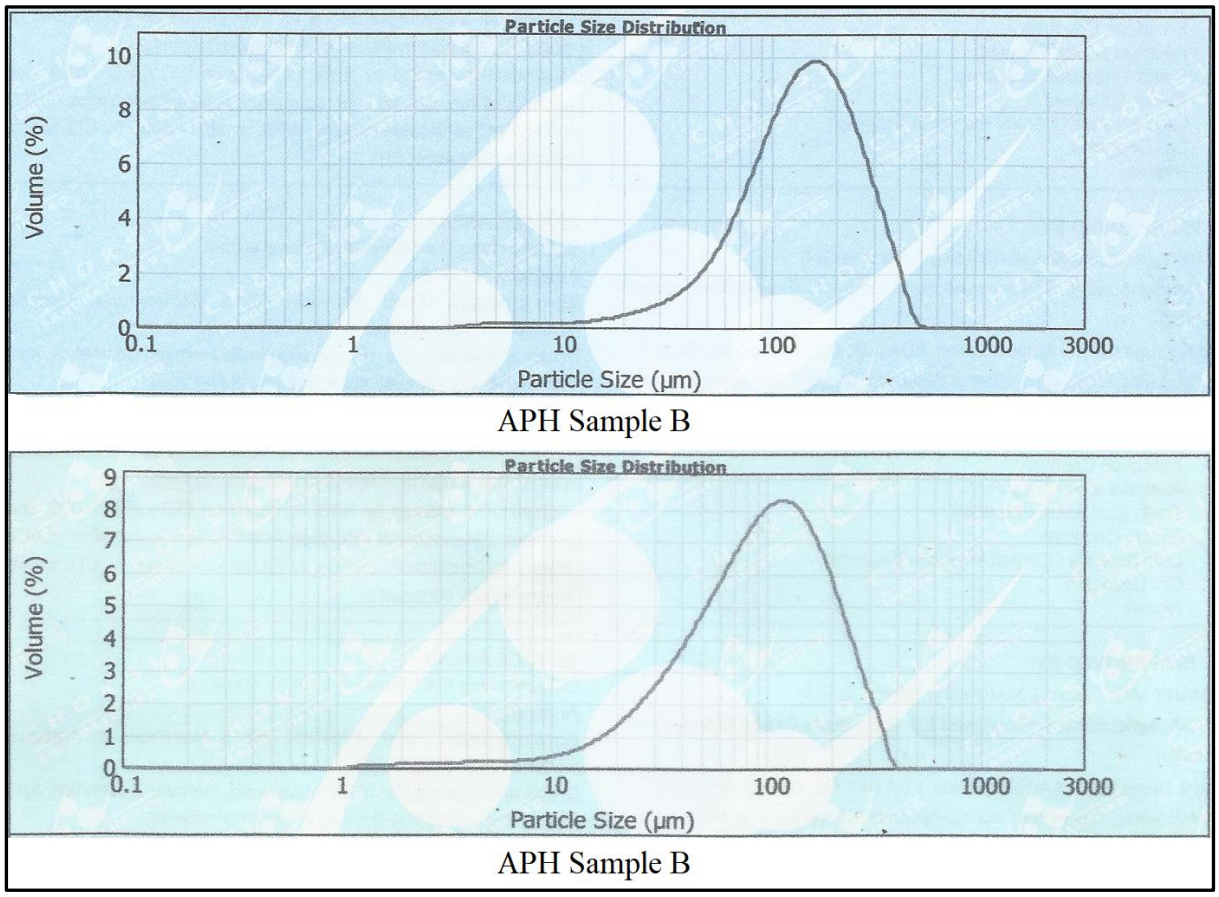

Figure 4.1: Particle size distribution of APH sample A and APH sample B fly ash

Morphological study of SEM images shown in Figure 4.1 results that both APH ash sample A and APH ash sample B consists of small, medium, and large size particles. APH ash sample A particles are more spherical than APH ash sample B but at the same more agglomeration than sample B ash. Figure 4.2 shows no significant difference between particle shapes of both the fly ash samples.

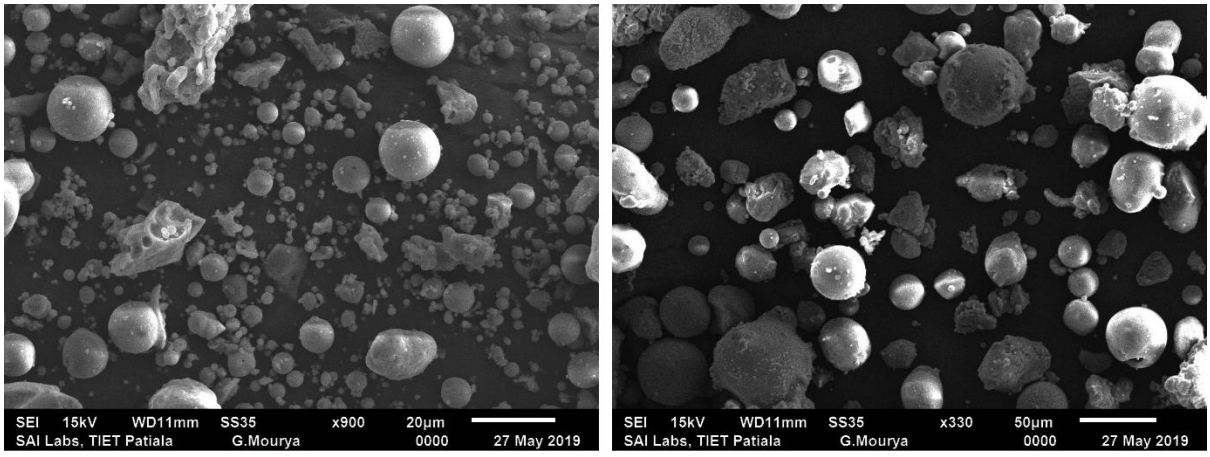

Figure 4.2: SEM pictures of APH ash sample A and APH ash sample B

4.2 Flow properties

Figure 4.3 shows flow function curves for APH ash sample A and APH ash sample B with Jenike's classification flow function curves (Schulze, 2008). The results show that major principle consolidation stress value more than 1.074kPa, APH sample B fly ash is in easy flowing zone and for major principle consolidation value more than 3.3kPa, APH sample A fly ash comes in the easy flowing zone. Below these respective values of consolidation stress, both samples are in the cohesive zone. Figure 4.3 also shows that these fly ash samples shows easy flowability at higher values of consolidation stress.

Figure 4.4 shows the effective angle of internal friction at different major consolidation stress values for APH sample A, and APH sample B fly ash. APH sample A fly ash shows the higher value of effective angle of internal friction as compared to APH sample B fly ash. As APH sample A ash is more cohesive than APH sample B, can be the reason for the higher value of internal friction angle.

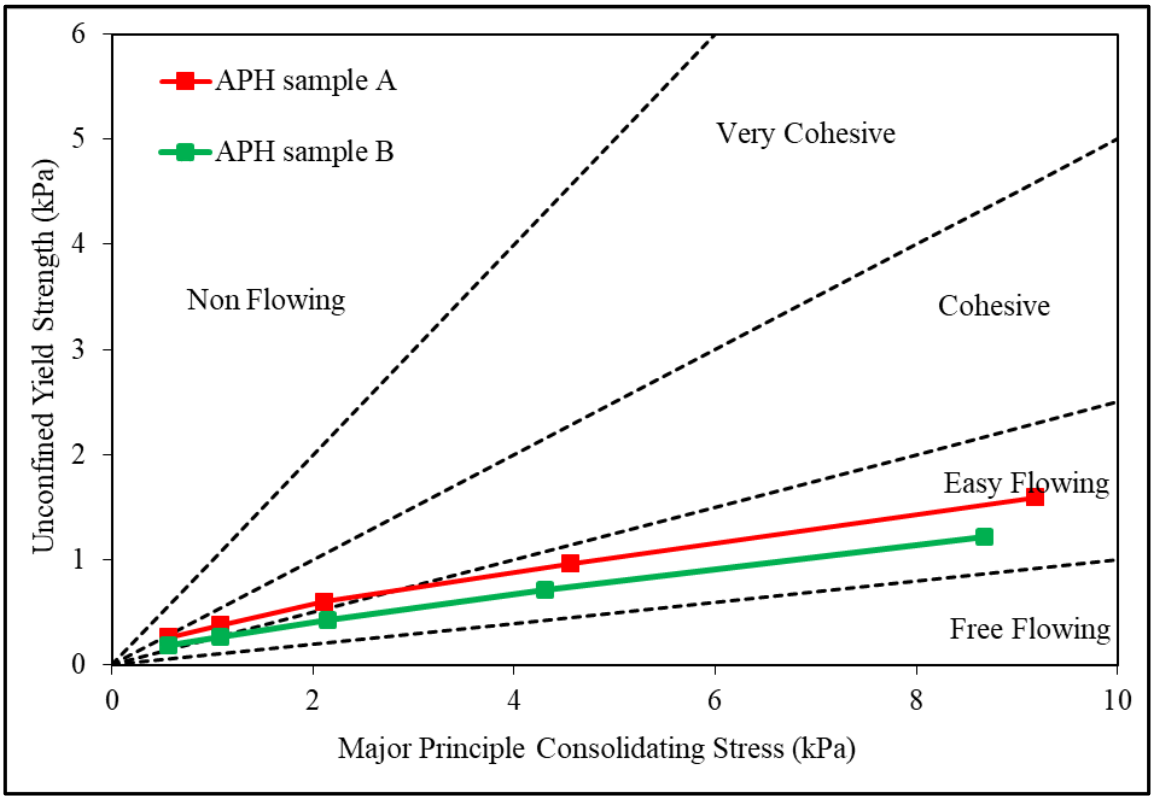

Figure 4.3: Flow function curve for APH sample A and APH sample B fly ash

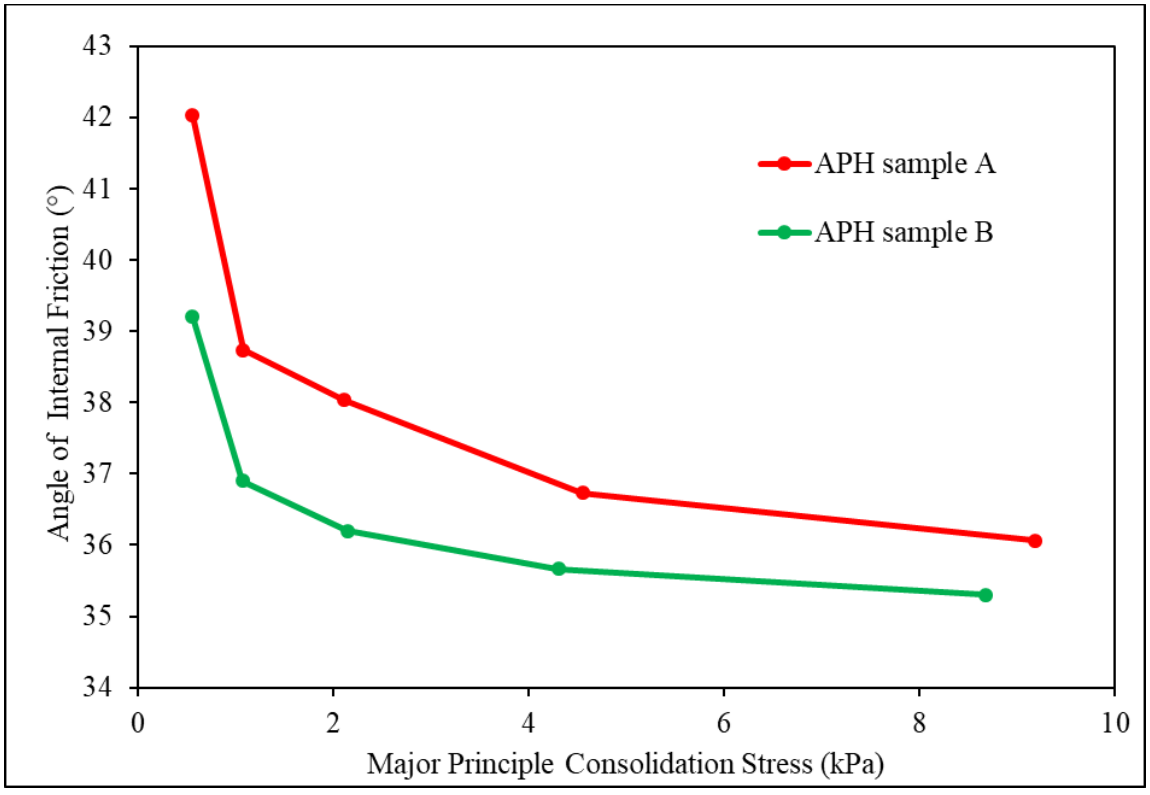

Figure 4.4: Variation of effective angle of internal friction with major principle consolidation stress for APH sample A and APH sample B fly ash

Figure 4.5 shows an effective angle of wall friction at different values of normal stress for APH sample A and APH sample B. APH sample A has higher value of effective wall friction angle than APH sample B fly ash for normal stress values less than 3kPa. For normal stress values higher than 3kPa, both APH sample A and APH sample B has approximately the same value of effective angle of wall friction. Table 4.2 contains experimental results for an effective angle of wall friction at different values of normal stress varying from 0.4 to 4.8 kPa.

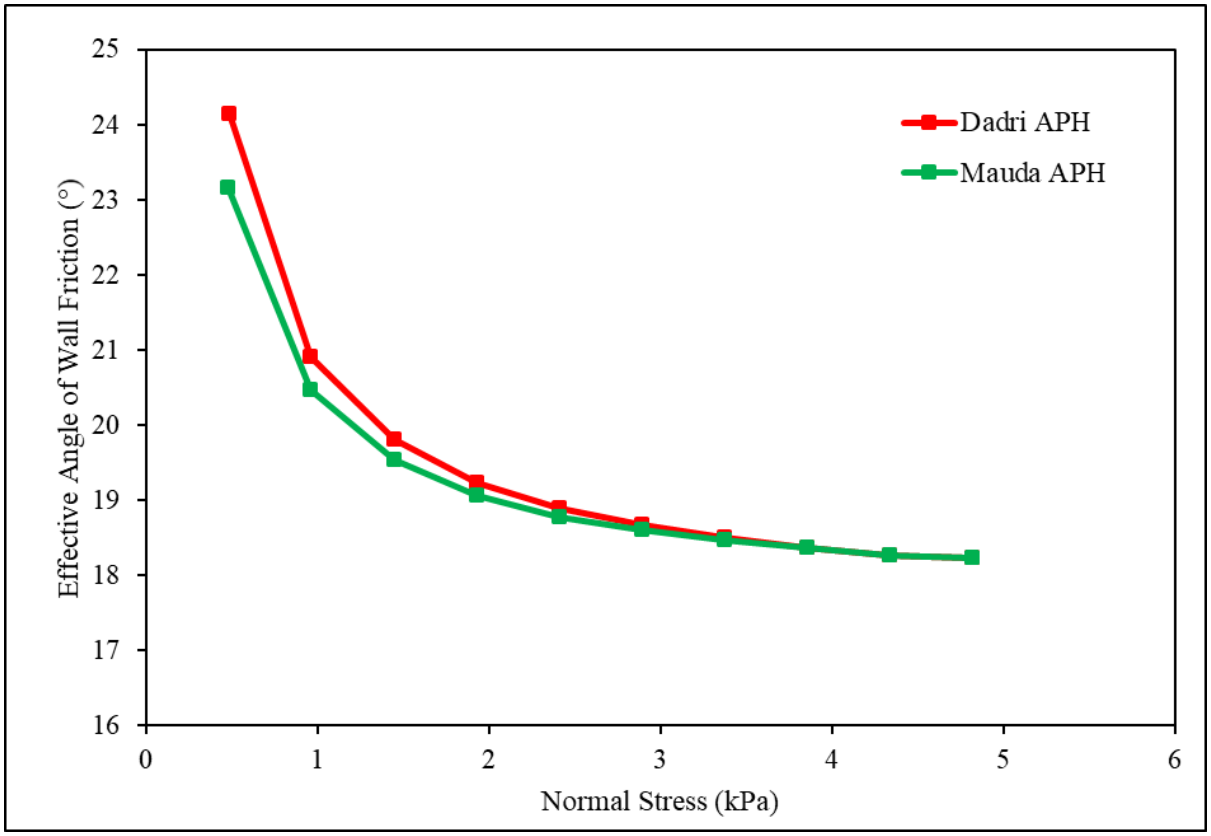

Figure 4.5: Variation of effective angle of wall friction with normal stress for APH sample A and APH sample B fly ash

Figure 4.6 shows the bulk density of APH sample A and APH sample B fly ash for different values of normal stress. Bulk density of APH sample A fly ash is higher than APH sample B fly ash. The slope of bulk density curve for APH sample A fly ash is higher than sample B fly ash, which can be due to higher porosity and compressibility index. Table 4.3 shows experimental results for bulk density at different values of normal stress.

Table 4.2: Experimental value of effective angle of wall friction at different normal stress values for APH sample A and APH sample B fly ash

Normal Stress (kPa)	Effective Angle of Wall Friction (°)	Effective Angle of Wall Friction (°)
	APH sample A	APH sample B
0.483	24.1	23.2
0.963	20.9	20.5
1.446	19.8	19.5
1.929	19.2	19.1
2.41	18.9	18.8
2.892	18.7	18.6
3.374	18.5	18.5
3.855	18.4	18.4
4.337	18.3	18.3
4.817	18.2	18.2

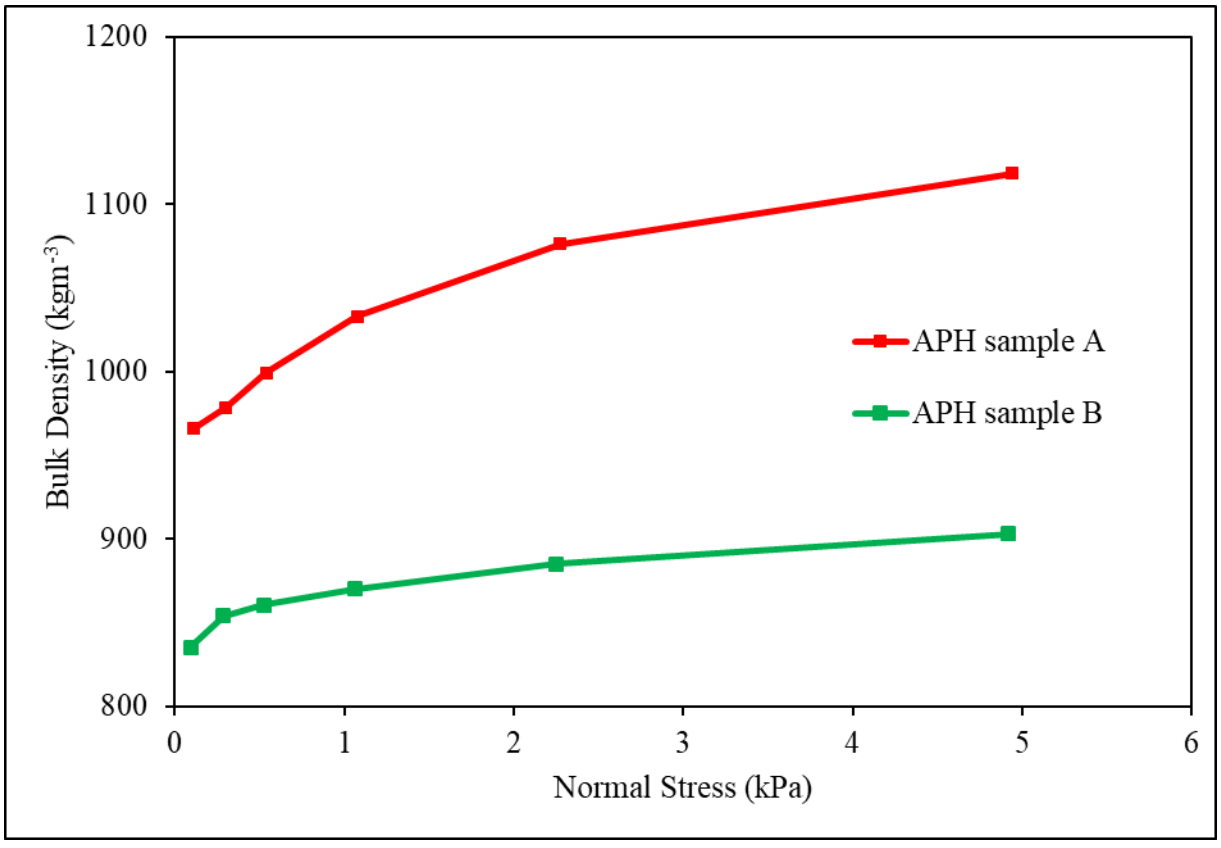

Figure 4.6: Variation of bulk density at different normal stress values for APH sample A and APH sample B fly ash

Table 4.3: Experimental results for bulk density at different normal stress values for APH sample A and APH sample B fly ash

APH sample A		APH sample B	
Normal Stress (kPa)	**Bulk Density (kg/m³)**	**Normal Stress (kPa)**	**Bulk Density (kg/m³)**
0.107	965.8	0.0923	835.1
0.299	978.6	0.2863	853.9
0.54	999.2	0.525	860.2
1.077	1032.7	1.059	869.8
2.272	1076.2	2.252	885.1
4.941	1118.2	4.918	903.1

Figure 4.7 shows time consolidated flow function curves for APH sample A and APH sample B fly ash, along with curves for Jenike's classification. After time consolidation, there is slight decline in flowability of both the APH samples A and B. After applying normal stress for sufficient time (12 hours in this experiment), compaction of fly ash takes place and inter-particle space reduces. More particles will be in contact with each other and fly ash become more cohesive that results in a reduction in flowability (Maltby, 1995).

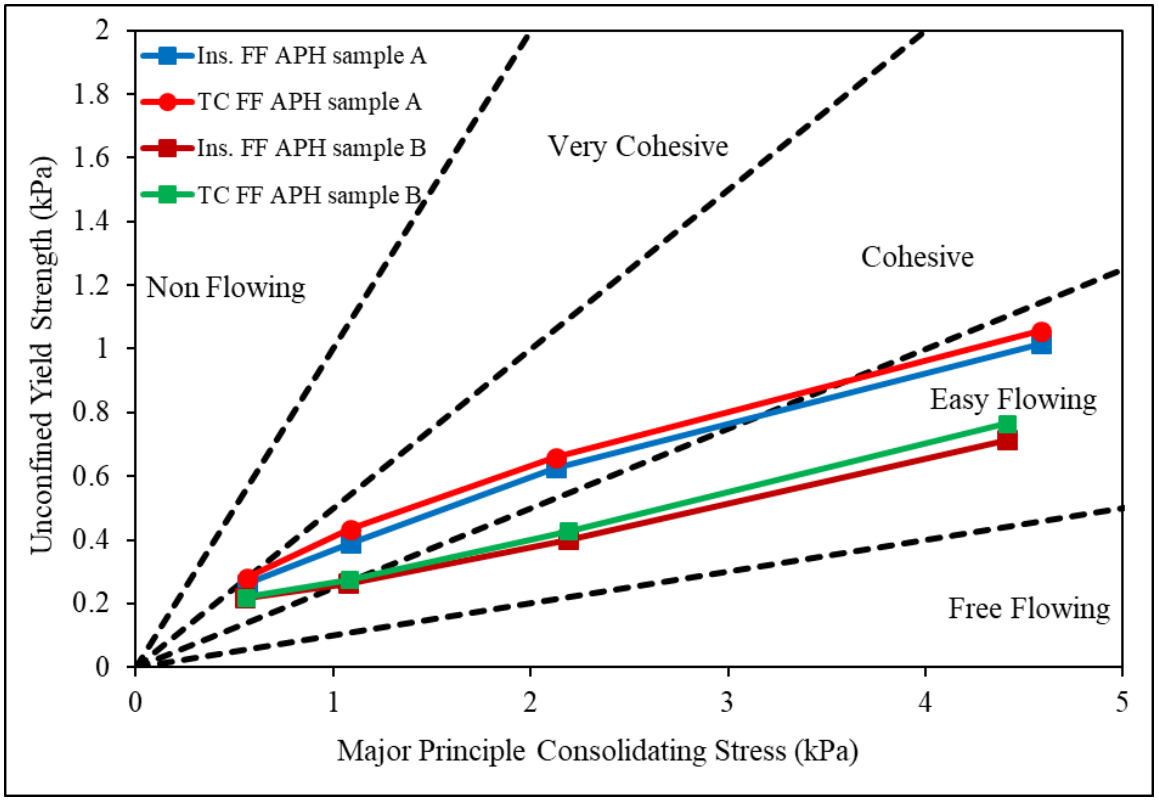

Figure 4.7: Time consolidated flow function curve for APH sample A and APH sample B fly ash

Table 4.4: Experimental results of flow function test for APH sample A and APH sample B fly ash

σ1 (kPa)	σc (kPa)	
	Instantaneous	Time consolidated
APH sample A		
0.564	0.262	0.281
1.085	0.389	0.434
2.126	0.626	0.658
4.583	1.016	1.057
APH sample B		
0.558	0.216	0.22
1.081	0.264	0.274
2.191	0.399	0.428
4.415	0.714	0.765

4.3 Hopper designing and fabrication for mass flow

For designing any hopper, there are two main design parameters, i.e. hopper half angle and critical outlet diameter. According to Schulze (2008), these design parameters can determined from the flow properties of the respective powder. Flow properties which required for determining hopper half angle are an effective angle of internal friction (δ_i) and wall friction angle (φ_w). Flow properties which required for determining critical outlet diameter are unconfined failure strength (σ_c) and compacted bulk density (σ_b).

These all properties have been determined with the help of PFT as already discussed. Formulae used for determining critical outlet diameter and hopper half angle are as follows:-

$$D_c = \frac{2.\sigma_c.1000}{\rho_b.g} \tag{4.1}$$

$$\theta = \left[90 - \frac{1}{2}.\cos^{-1}\left(\frac{1-\sin\delta}{2.\sin\delta}\right)\right] - \frac{1}{2}\left[\varphi_w + \sin^{-1}\left(\frac{\sin\varphi_w}{\sin\delta}\right)\right] \tag{4.2}$$

Figure 4.8 and Figure 4.9 shows design parameters that are hopper half angle and hopper outlet diameter for conical and trapezoidal hoppers. Conical hopper design for same fly ash sample requires a larger hopper half angle for constant hopper outlet dimension. Table 4.5 shows experimental for hopper half angle and hopper outlet diameter. For APH sample A fly ash hopper half angle required is lesser as compared to APH sample B fly ash. That can be due to a higher effective angle of wall friction and higher effective angle of wall friction than APH sample A.

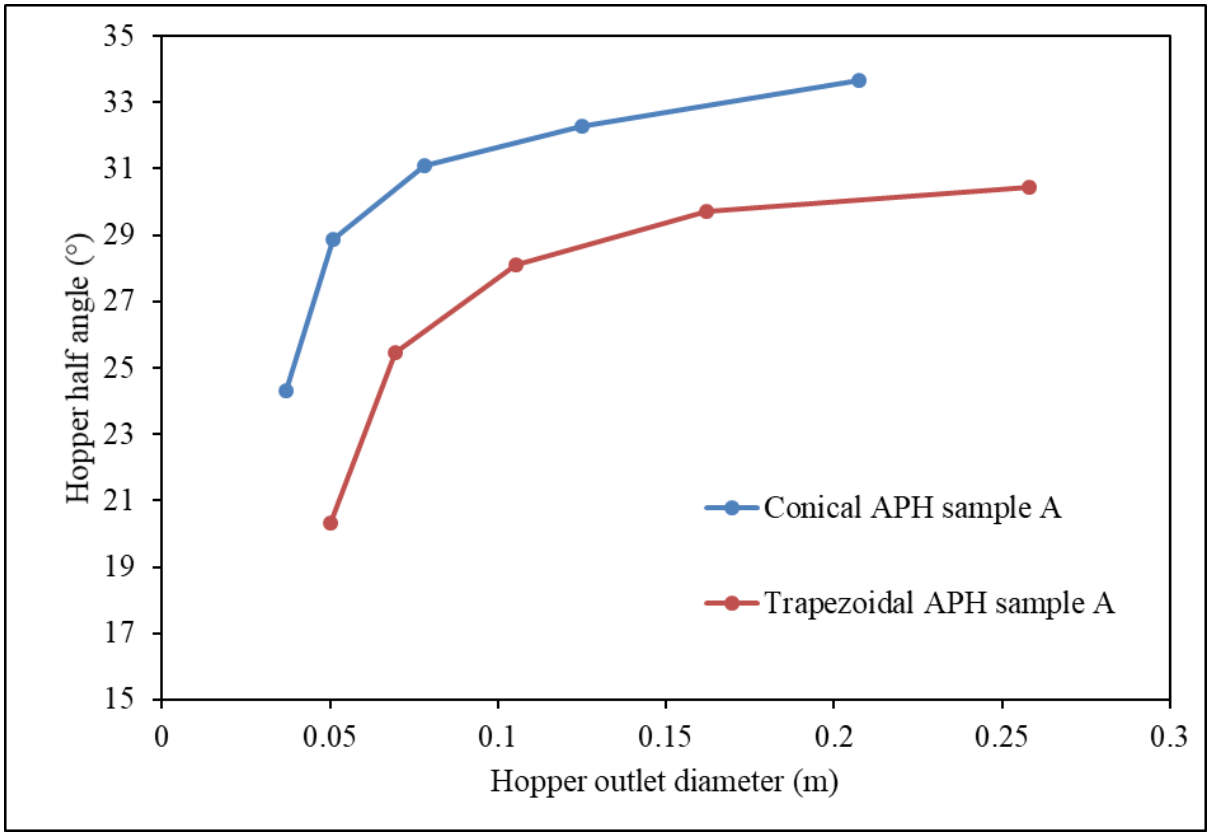

Figure 4.8: Conical and trapezoidal hopper half angle variation with hopper outlet diameter for APH sample A fly ash

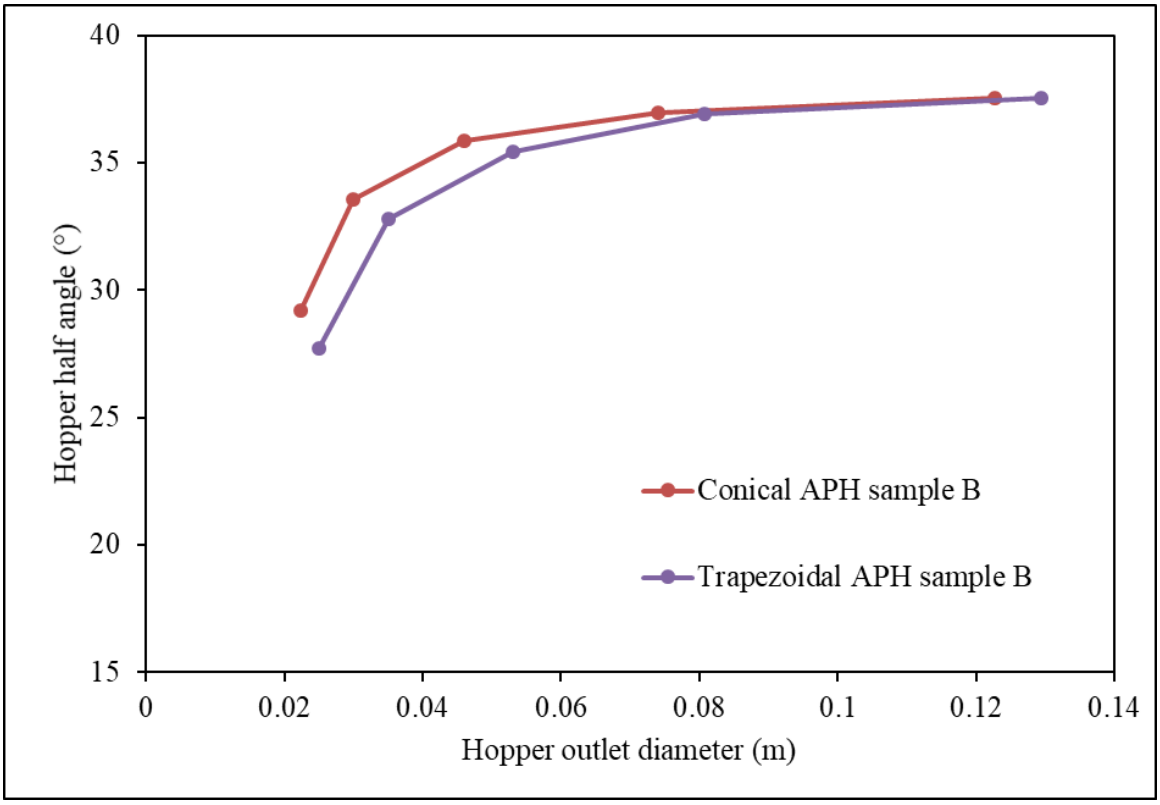

Figure 4.9: Conical and trapezoidal hopper half angle variation with hopper outlet diameter for APH sample B fly ash

Table 4.5: Experimental results for conical and trapezoidal hopper half angle at different hopper outlet diameters for APH sample A and APH sample B fly ash

APH sample A		**APH sample B**	
Hopper outlet diameter (m)	**Hopper half angle (°)**	**Hopper outlet diameter (m)**	**Hopper half angle (°)**
Conical hopper			
0.037	24.3	0.0223	29.2
0.051	28.8	0.03	33.5
0.078	31.1	0.046	35.8
0.125	32.3	0.074	36.9
0.207	33.7	0.123	37.5
Trapezoidal hopper			
0.0503	20.3	0.025	27.7
0.0693	25.4	0.035	32.8
0.105	28.1	0.053	35.4
0.162	29.7	0.0806	36.9
0.258	30.4	0.129	37.5

Fig. 4.11 shows manufactured conical and trapezoidal hoppers. Manufacturing of these hoppers mainly included two phases, designing, and fabrication. Designing procedure as already discussed above. Fabrication of these hoppers included various operations, i.e. metal sheet cutting, welding, bending, and checking dimension accuracy. For fabrication, sheets of Mild steel AISI 1018 of thickness 3mm has used. Metal inert gas (MIG) welding has used for the high quality weld.

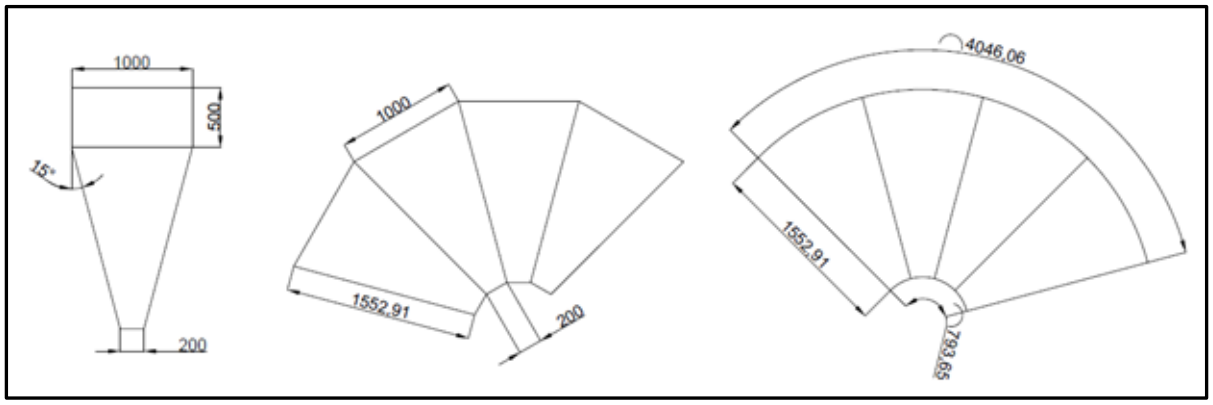

Figure 4.10: Development drawing of Conical and trapezoidal hopper on Autodesk AutoCAD 2015

Figure 4.11: Picture of fabricated trapezoidal (left) and conical (right) hoppers

4.4 Modelling solid friction factor

Readings noted from data logger connected to load cells analysed. There was a large amount of data generated during experimentation as readings noted at the rate of 1 reading/ 5 sec. The raw data has been cropped to get only useful data. Figure 4.12 shows the plot of load cell for the transfer hopper vs time. The graph shows the decreasing value of load cell reading with time, which indicates the transfer hopper has been unloading. From this graph, the solid mass flow has calculated. For each experiment, a similar procedure has repeated for calculating solid mass flow rate as shown in Table 6.1.

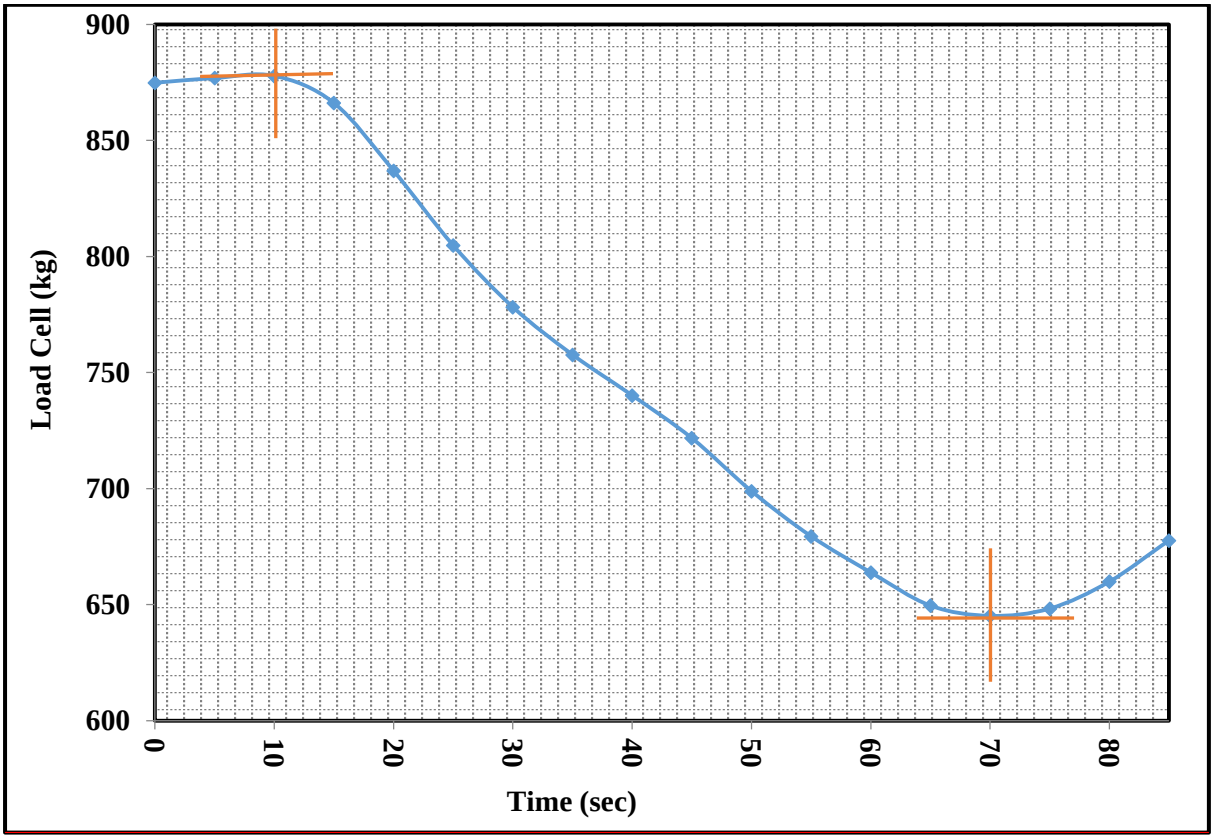

Figure 4.12: Data logger reading for transfer hopper load cell

Table 4.6: Experimental readings for solid mass flow rate in vacuum conveying system

Ex. No.	Initial load	Final load	Initial time	Final time	Mass flow rate (kg/sec)
1	1033	896	210	310	1.37
2	969.4	831.5	70	105	3.94
3	931.8	714.3	20	55	6.21
4	877.8	645.1	30	90	3.88
5	1039.6	817.5	15	75	3.70
6	936.9	741.5	40	95	3.55
7	870.6	683.9	45	100	3.39
8	815.2	607.3	10	60	4.16
9	986.5	735.7	20	55	7.16

The new model has developed for predicting solid friction factor. For modeling, solid friction factor taken as a function of solid loading ratio and gas Froude number. Solid loading ratio is the ratio of the mass flow rate of solid to the mass flow rate of air or gas, which signifies the proportion of solid conveyed for air supply. Gas Froude number signifies relative inertial effect for gravitational effect.

Format for modeling solid friction factor is as equation (4.3) –

$$\lambda_s = K.(m^*)^a.(Fr_g)^b \tag{4.3}$$

Experimental values of solid friction factor, mass flow rate and Froude number has been used to develop a new model. Microsoft Excel 2016 has used, and by applying multiple regression got values of coefficients K, a and b as mentioned in equation (4.4) –

$$\lambda_s = 1.(m^*)^{-0.2378}.(Fr_g)^{-.14546} \tag{4.4}$$

Table 4.7: Percentage relative error for predicted solid friction factor

Ex. No.	Fr_g	m^*	Experimental value of λ_s	Predicted value of λ_s	Percentage relative error
1	19.23	26.307	0.0057	0.0062	8.6%
2	19.71	16.021	0.0081	0.0068	16.5%
3	20.46	14.730	0.0069	0.0065	5%
4	20.36	14.209	0.0074	0.0066	10.05%
5	20.70	13.352	0.0070	0.0066	5.9%
6	20.49	16.519	0.0061	0.0063	4.6%
7	17.73	32.902	0.0062	0.0066	8%

Values of solid friction factor predicted for experimental setup shown in Fig. 3.3 is shown in table 4.7. It is shown that the new model developed predicted with high accuracy. Curve fitting for plot between predicted solid friction factor and experimental solid friction factor gives R^2 value.

Value of 0.9907 proved the accuracy of the developed model, as shown in Fig. 4.13.

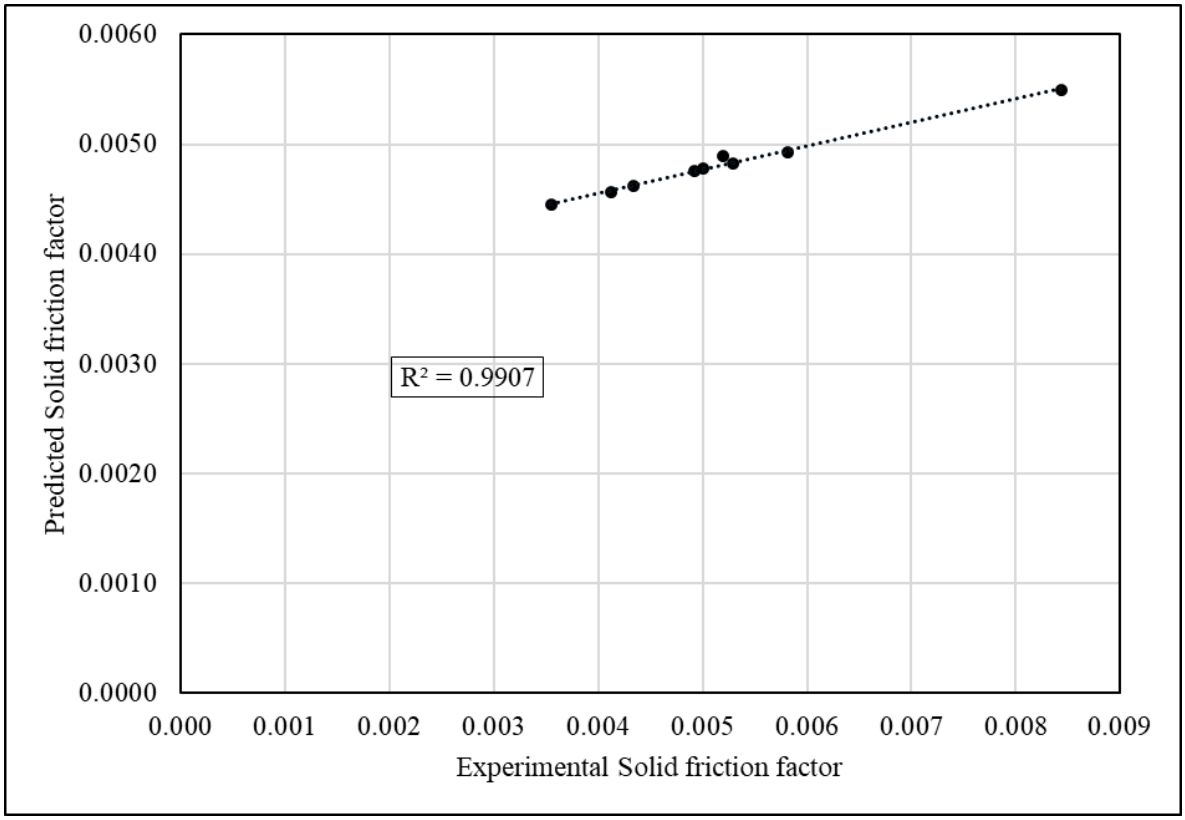

Figure 4.13: Plot between Experimental and Predicted solid friction factor

Chapter 5

Conclusion and Future Scope

5.1 Conclusion

APH ash sample B is more easily flowing than APH ash sample A. This can be due to higher porosity, Hausner ratio, and compressibility index of APH sample A. Sample A fly ash requires higher outlet diameter value than sample B fly ash. The reason behind that can be higher internal friction angle, and higher wall friction angle of sample A fly ash than sample B fly ash. It can said that the hopper which is suitable for conveying APH sample B fly ash might show flow problems for APH sample A fly ash. Time consolidation shows some effect on the flowability of both sample B and sample A fly ash. After storing these samples under constant stress for 12 hours results decline in flowability. It can said that hopper designed for the instantaneous flow may show flow problems after storing powder for more than 12 hours. If the only particle size taken into consideration, flowability decreases with decrease in particle size (Lee et al., 2015). APH sample A has a larger particle size shown lower flowability than APH sample B. This can be concluded that there are also other factors like porosity, compressibility index, and Hausner ratio that influence flowability.

Standard methods need to follow for designing any hopper. Different physical properties and flow properties must be analyzed thoroughly for hopper designing. Time consolidation test showed the importance for designing hopper as a change in flow properties noted after storage of bulk solids. Model for solid friction factor has developed from experimental results of vacuum conveying setup.

5.2 Future scope

An attempt was made to follow a procedure to determine hopper geometry and develop a model for solid friction factor. There is a lot of future scope and work that can done as flowing -

- The testing facility can developed for analyzing the effect of storage of bulk solids over an extensive period more than one month.
- The model developed for solid friction factor is dependent on solid loading ratio and gas Froude number. There can be other factors that can be included to model more accurately.
- The model developed can be validated for a variety of bulk solids, different parameters, and scale-up conditions.

REFERENCES

Rohit, A.K., Devi, K.P. and Rangnekar, S., 2017. An overview of energy storage and its importance in Indian renewable energy sector: Part I–Technologies and Comparison. *Journal of Energy Storage*, *13*, pp.10-23.

Salehi, H., Barletta, D. and Poletto, M., 2017. A comparison between powder flow property testers. *Particuology*, *32*, pp.10-20.

Klinzing, G.E., Rizk, F., Marcus, R. and Leung, L.S., 2011. *Pneumatic conveying of solids: a theoretical and practical approach* (Vol. 8). Springer Science & Business Media.

Schulze, D., 2008. Powders and bulk solids. *Behaviour, Characterization, Storage and Flow. Springer*, pp.35-74.

Geldart, D., 1973. Types of gas fluidization. *Powder technology*, *7*(5), pp.285-292.

Garg, V., Mallick, S.S., Garcia-Trinanes, P. and Berry, R.J., 2018. An investigation into the flowability of fine powders used in pharmaceutical industries. *Powder technology*, *336*, pp.375-382.

Bian, Q., Sittipod, S., Garg, A. and Ambrose, R.K., 2015. Bulk flow properties of hard and soft wheat flours. *Journal of Cereal Science*, *63*, pp.88-94.

Takeuchi, Y., Tomita, T., Kuroda, J., Kageyu, A., Yonekura, C., Hiramura, Y., Tahara, K. and Takeuchi, H., 2018. Characterization of mannitol granules and powder: A comparative study using two flowability testers. *International journal of pharmaceutics*, *547*(1-2), pp.106-113.

Rohilla, L., Garg, V., Mallick, S.S. and Setia, G., 2018. An experimental investigation on the effect of particle size into the flowability of fly ash. *Powder Technology*, *330*, pp.164-173.

Lee, Y.J. and Yoon, W.B., 2015. Flow behavior and hopper design for black soybean powders by particle size. *Journal of Food Engineering*, *144*, pp.10-19.

Fitzpatrick, J.J., Barringer, S.A. and Iqbal, T., 2004. Flow property measurement of food powders and sensitivity of Jenike's hopper design methodology to the measured values. *Journal of Food Engineering*, *61*(3), pp.399-405.

Leung, L.Y., Mao, C., Chen, L.P. and Yang, C.Y., 2016. Precision of pharmaceutical powder flow measurement using ring shear tester: High variability is inherent to powders with low cohesion. *Powder Technology*, *301*, pp.920-926.

Mallick, S.S. and Wypych, P.W., 2009. Minimum transport boundaries for pneumatic conveying of powders. *Powder Technology*, *194*(3), pp.181-186.

Setia, G. and Mallick, S.S., 2015. Modelling fluidized dense-phase pneumatic conveying of fly ash. *Powder technology*, *270*, pp.39-45.

Setia, G., Mallick, S.S., Pan, R. and Wypych, P.W., 2015. Modeling minimum transport boundary for fluidized dense-phase pneumatic conveying systems. *Powder technology*, *277*, pp.244-251.

Cabrejos, F.J. and Klinzing, G.E., 1994. Pickup and saltation mechanisms of solid particles in horizontal pneumatic transport. *Powder technology*, *79*(2), pp.173-186.

Wypych, P.W. and Yi, J., 2003. Minimum transport boundary for horizontal dense-phase pneumatic conveying of granular materials. *Powder Technology*, *129*(1-3), pp.111-121.

Kalman, H., Satran, A., Meir, D. and Rabinovich, E., 2005. Pickup (critical) velocity of particles. *Powder Technology*, *160*(2), pp.103-113.

Zhou, J.W., Du, C.L. and Ma, Z.L., 2018. Influence of swirling intensity on lump coal particle pickup velocity in pneumatic conveying. *Powder technology*, *339*, pp.470-478.

Hu, S., Zhou, F., Geng, F., Liu, Y., Zhang, Y. and Wang, Q., 2014. Investigation on blockage boundary condition of dense-phase pneumatic conveying in bending slits. *Powder technology*, *266*, pp.96-105.

Hu, S., Zhou, F., Liu, Y., Kang, J., Zhang, Y. and Xia, T., 2015. Experimental study of the blockage boundary for dense-phase pneumatic conveying of powders through a horizontal slit. *Particuology*, *21*, pp.128-134.

Cenna, A.A., Williams, K.C., Jones, M.G. and Robinson, W., 2014. Analysis of wear mechanisms in pneumatic conveying pipelines of fly ash. In *Engineering Asset Management 2011*(pp. 539-547). Springer, London.

Pan, R., 1999. Material properties and flow modes in pneumatic conveying. *Powder technology*, *104*(2), pp.157-163.

Rabinovich, E. and Kalman, H., 2011. Flow regime diagram for vertical pneumatic conveying and fluidized bed systems. *Powder Technology*, *207*(1-3), pp.119-133.

Abdullah, E.C. and Geldart, D., 1999. The use of bulk density measurements as flowability indicators. *Powder technology*, *102*(2), pp.151-165.

Carr, R.L., 1965. Evaluating flow properties of solids.

Jenike, A.W., 1964. Storage and Flow of Solids, Bull, No. 123. *Bull. Univ*. Schulze, D., 1990. Standard shear testing technique for particulate solids using the Jenike shear cell: edited by The Institution of Chemical Engineers, Rugby, UK, 1989; 46 pp. paperback;£ 16.50 plus postage; ISBN 0 85295 232 5.

Barbosa-Cánovas, G.V., Ortega-Rivas, E., Juliano, P. and Yan, H., 2005. *Food powders: physical properties, processing, and functionality* (Vol. 86, pp. 71-75). New York: Kluwer Academic/Plenum Publishers.

Maltby, L.P., Enstad, G.G. and de Selva, S.R., 1995. Investigation of the behaviour of powders under and after consolidation. *Particle & particle systems characterization*, *12*(1), pp.16-27.8

Harpreet Thesis 15-07-19

ORIGINALITY REPORT

11%	4%	10%	6%
SIMILARITY INDEX	INTERNET SOURCES	PUBLICATIONS	STUDENT PAPERS

PRIMARY SOURCES

1	Vivek Garg, S.S. Mallick, Pablo Garcia-Trinanes, Robert James Berry. "An investigation into the flowability of fine powders used in pharmaceutical industries", Powder Technology, 2018 Publication	1%
2	Lokesh Rohilla, Vivek Garg, S.S. Mallick, Gautam Setia. "An experimental investigation on the effect of particle size into the flowability of fly ash", Powder Technology, 2018 Publication	1%
3	G. Setia, S.S. Mallick, R. Pan, P.W. Wypych. "Modeling minimum transport boundary for fluidized dense-phase pneumatic conveying systems", Powder Technology, 2015 Publication	1%
4	S. S. Mallick, Lokesh Rohilla, Vivek Garg, Gautam Setia. "Modeling flow properties of fine dry powders using particle morphological properties and its effects on geometry of fly ash evacuation hoppers", Particulate Science and	<1%

Technology, 2018
Publication

5	Bulk Solids Handling, 1987. Publication	<1%
6	Hamid Salehi, Nicoletta Lotrecchiano, Diego Barletta, Massimo Poletto. "Dust Release from Aggregative Cohesive Powders Subjected to Vibration", Industrial & Engineering Chemistry Research, 2017 Publication	<1%
7	Shengyong Hu, Fubao Zhou, Yingke Liu, Jianhong Kang, Yifan Zhang, Tongqiang Xia. "Experimental study of the blockage boundary for dense-phase pneumatic conveying of powders through a horizontal slit", Particuology, 2015 Publication	<1%
8	Submitted to University of Sheffield Student Paper	<1%
9	Yoshiko Takeuchi, Tomoka Tomita, Junko Kuroda, Akihiro Kageyu et al. "Characterization of mannitol granules and powder: A comparative study using two flowability testers", International Journal of Pharmaceutics, 2018 Publication	<1%
10	Youn Ju Lee, Won Byong Yoon. "Flow behavior and hopper design for black soybean powders	<1%

by particle size", Journal of Food Engineering, 2015
Publication

11	www.brookfieldengineering.uk Internet Source	<1%
12	Submitted to University of New South Wales Student Paper	<1%
13	Particle Technology Series, 2016. Publication	<1%
14	Submitted to University of Leeds Student Paper	<1%
15	www.answers.com Internet Source	<1%
16	Saman Setoodeh Jahromy, Christian Jordan, Mudassar Azam, Andreas Werner, Michael Harasek, Franz Winter. "Fly ash from municipal solid waste incineration as a potential thermochemical energy storage", Energy & Fuels, 2019 Publication	<1%
17	Submitted to Central Queensland University Student Paper	<1%
18	Submitted to University of Greenwich Student Paper	<1%

www.uniassignment.com

19	Internet Source	<1%
20	dspace.thapar.edu:8080 Internet Source	<1%
21	www.fst.ohio-state.edu Internet Source	<1%
22	G.E. Klinzing, F. Rizk, R. Marcus, L.S. Leung. "Pneumatic Conveying of Solids", Springer Science and Business Media LLC, 2010 Publication	<1%
23	Kulsum Jan, C. S. Riar, D. C. Saxena. "Value addition to agro industrial by-products: Effect of temperature and plasticizer on various properties of pellets developed using extrusion technology", Journal of Food Processing and Preservation, 2017 Publication	<1%
24	Shengyong Hu, Fubao Zhou, Fan Geng, Yingke Liu, Yifan Zhang, Qingxiang Wang. "Investigation on blockage boundary condition of dense-phase pneumatic conveying in bending slits", Powder Technology, 2014 Publication	<1%
25	www.alp.gov.pk Internet Source	<1%
	upcommons.upc.edu	

26	Internet Source	<1%
27	Kapil Sharma, Soumya. S. Mallick, Anu Mittal, Peter Wypych. "Modelling solids friction for fluidized dense-phase pneumatic conveying", Particulate Science and Technology, 2019 Publication	<1%
28	Fitzpatrick, J.. "Effect of powder properties and storage conditions on the flowability of milk powders with different fat contents", Journal of Food Engineering, 200410 Publication	<1%
29	Submitted to Karunya University Student Paper	<1%
30	Submitted to (school name not available) Student Paper	<1%
31	www.ijert.org Internet Source	<1%
32	James M. Craven, Jim Swithenbank, Vida N. Sharifi. "Investigation into the Flow Properties of Coarse Solid Fuels for Use in Industrial Feed Systems", Journal of Powder Technology, 2015 Publication	<1%
33	Setia, G., and S.S. Mallick. "Modelling fluidized dense-phase pneumatic conveying of fly ash", Powder Technology, 2015.	<1%

	Publication	
34	Submitted to South Dakota Board of Regents Student Paper	<1%
35	A Ye. "Influence of calcium chloride addition on the properties of emulsions stabilized by whey protein concentrate", Food Hydrocolloids, 2000 Publication	<1%
36	Submitted to Glasgow Caledonian University Student Paper	<1%
37	www.scribd.com Internet Source	<1%
38	Erol, M.. "Characterization of sintered coal fly ashes", Fuel, 200806 Publication	<1%
39	espace.curtin.edu.au Internet Source	<1%
40	docplayer.net Internet Source	<1%
41	Naveen Tripathi, Atul Sharma, S.S. Mallick, P.W. Wypych. "Energy loss at bends in the pneumatic conveying of fly ash", Particuology, 2015 Publication	<1%
42	ijrer.org Internet Source	<1%

43	Submitted to University of Hong Kong Student Paper	<1%
44	Submitted to University of Birmingham Student Paper	<1%
45	Submitted to Curtin University of Technology Student Paper	<1%
46	Submitted to University of Edinburgh Student Paper	<1%
47	Submitted to Cork Institute of Technology Student Paper	<1%
48	tel.archives-ouvertes.fr Internet Source	<1%
49	Naveen Mani Tripathi, Nir Santo, Haim Kalman, Avi Levy. "Experimental analysis of particle velocity and acceleration in vertical dilute phase pneumatic conveying", Powder Technology, 2018 Publication	<1%
50	G. Setia, S.S. Mallick, P.W. Wypych. "On improving solid friction factor modeling for fluidized dense-phase pneumatic conveying systems", Powder Technology, 2014 Publication	<1%
51	dspace.ewubd.edu Internet Source	<1%

52	Submitted to British University in Egypt Student Paper	<1%
53	Fei Yan, Akira Rinoshika. "High-speed PIV measurement of particle velocity near the minimum air velocity in a horizontal self-excited pneumatic conveying of using soft fins", Experimental Thermal and Fluid Science, 2013 Publication	<1%
54	Mills, . "Types of Pneumatic Conveying Systems", Dekker Mechanical Engineering, 2004. Publication	<1%

Exclude quotes	On	Exclude matches	< 8 words
Exclude bibliography	On		